LOCAL ADAPTIVE SLICING FOR LAYERED MANUFACTURING

Justin T. Tyberg

Thesis submitted to the Faculty of the Virginia Polytechnic Institute and State University in partial fulfillment of the requirements for the degree of

Master of Science
in
Mechanical Engineering

Jan Helge Bøhn, Chair
Arvid Myklebust
Ronald Kander

February 16, 1998
Blacksburg, Virginia

Keywords: Adaptive Slicing, Calibration, Contour Matching, Fused Deposition Modeler (FDM)

LOCAL ADAPTIVE SLICING FOR LAYERED MANUFACTURING

by

Justin Tyberg

Jan Helge Bøhn, Chairman

Department of Mechanical Engineering

ABSTRACT

Existing layered manufacturing systems fabricate parts using a constant build layer thickness. Hence, operators must compromise between rapid production with large surface inaccuracies, and slow production with high precision, by choosing between thick and thin build layers, respectively. Adaptive layered manufacturing methods alleviate this decision by automatically adjusting the build layer thickness to accommodate surface geometry, thereby potentially enabling part fabrication in significantly less time. Unfortunately, conventional adaptive layered manufacturing techniques are often unable to realize this potential when transitioning from the laboratory to an industrial setting. The problem is that they apply the variable build layer thickness uniformly across each horizontal build plane, applying the same build layer thickness to all parts and part features across that plane even though they have different build layer thickness needs. When this happens, the advantage of using adaptive build layer thicknesses is lost. This thesis demonstrates how to minimize fabrication times when implementing adaptive layered manufacturing. Specifically, it presents a new method in which each part or individual part feature is assigned a distinct, independent build layer thickness according to its particular surface geometry. Additionally, this thesis presents a calibration procedure for the Fused Deposition Modeler (FDM) rapid prototyping system that enables accurate, adaptively sliced parts to be physically realizable. Experimental software has been developed and sample parts have been fabricated to demonstrate both aspects of this work.

ACKNOWLEDGEMENTS

I would like to extend thanks to the people whose contributions helped to make this thesis possible. In particular, I would like to thank:

- Dr. Jan Helge Bøhn, my advisor, for introducing me to the world of rapid prototyping, and for helping me discover the tools I needed to complete my research.
- Dr. Arvid Myklebust, committee member and Director of the Virginia Tech CAD Lab, for introducing me to the world of CAD/CAM, for making the mathematics of geometric curves and surfaces so interesting, and most of all, for providing me with a great experience as a CAD lab teaching assistant.
- Dr. Ron Kander, committee member, for explaining to me the fundamentals of the characteristics of polymer materials, and for being so flexible in scheduling.
- Darrell Early, Manager of the Virginia Tech CAD Lab, for his ability to remedy the seemingly abundant hardware and software problems so quickly.
- The Virginia Tech Department of Mechanical Engineering for funding me throughout my graduate career, and for providing ample computing resources.
- Stratasys, Inc., Eden Prairie, Minnesota for providing the Virginia Tech Rapid Prototyping Lab with outstanding service of its FDM 1600 rapid prototyping system.
- Bjarne Stroustrup and David R. Musser, for developing the C++ programming language and the Standard Template Library, respectively.

Finally, I would like to thank my fiancé, Christy, for her unending support through every stage of this work.

TABLE OF CONTENTS

LIST OF FIGURES

LIST OF TABLES

CHAPTER 1

INTRODUCTION

Rapid prototyping refers to a family of modern technologies in which three-dimensional, solid objects are fabricated under computer control. There are several advantages that these automated processes have which are absent from manual fabrication and molding processes. The most important is known as *Solid WYSIWYG* ("What-you-see-is-what-you-get"). Essentially this is the result of removing human interpretation, or error, from the manufacturing process. The object is designed and fabricated solely from computer data. Rapid prototyping also enables fast and frequent design iterations. Designers are able to fabricate physical prototypes that aid them in eliminating potential design flaws early in a product's development stages, leading to reduced production costs. Finally, rapid prototyping processes enable fabrication of parts with a high degree of accuracy.

Rapid prototyping processes fall into three categories: subtractive, formative, and additive. Subtractive processes achieve the desired shape of an object by successively removing material from an initial block of solid material. Examples of automated subtractive processes include computer numerical control (CNC) milling and wire-type electrical discharge machining (EDM). Formative processes apply mechanical forces to material to form it into a desired shape. Examples of this type of process are stamping, bending and forging. Additive processes build objects by adding successive layers of raw material to create a solid volume. Subtractive and formative processes are well established and understood. Additive processes, on the other hand, have emerged more recently. 3D Systems, Inc. introduced the first commercially available system, the Stereolithography Apparatus (SLA), in 1987. Since then, a myriad of additive processes has been introduced, including Fused Deposition Modeling (FDM), which was made available by Stratasys, Inc. in 1992 [Burns93].

The term *layered manufacturing* (LM) is commonly used to describe the family of modern additive processes. In these processes, the geometry of the object to be manufactured can be

obtained from computer aided design (CAD) model data, an existing object (through reverse engineering), or mathematical data (e.g., surface equations) [Burns93]. Regardless of the source, the geometry must be processed. First it is converted into a series of horizontal layers, whose thickness is often specified by the user. This is generally known as the slicing process. These layers are then used to generate the numerical control (NC) code required by the fabricator to build the corresponding physical layers. Most all LM fabrication systems accept CAD model data described in an intermediate file format called the .STL format. This file format approximates the original CAD model geometry by a series of triangular facets whose information can be easily processed by the LM hardware. A slicing procedure is then applied to the tessellated model. In this process, the model is intersected with a set of horizontal planes to create a series of cross sections, or slices, comprised of contours that represent the material boundaries of the part to be generated. The contours are subsequently used to generate the NC tool paths for the LM hardware.

Fabricating a freeform sculptured 3D geometry by a series of 2½D layers will inherently produce an approximate representation of the original surface geometry. This is commonly referred to as the stair-stepping effect, and it affects all non-horizontal surfaces. Figure 1.1 illustrates how the inaccuracies caused by the stair-stepping effect are considerably larger with thicker build layers. Conversely, the use of thinner build layers tends to provide smoother, more precise surfaces. Hence, the surface quality of a part can be improved by simply decreasing the build layer thickness. However, because both thick and thin layers have similar build times, reducing the build layer thickness will result in an increase in fabrication time. Herein lies the dilemma that is currently facing the rapid prototyping industry. Operators must choose a build layer thickness that will produce a part with an acceptable level of accuracy in an acceptable amount of time.

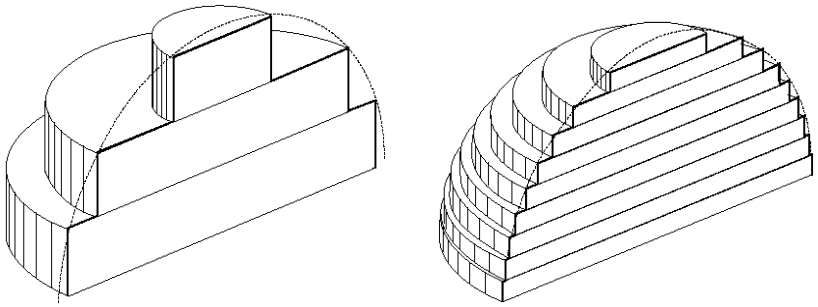

(a) (b)

Figure 1.1: Comparison of stair-stepping inaccuracies due to thick and thin build layers. (a) Thick build layers poorly approximate complex surfaces; (b) thin layers better approximate these surfaces; [Sabourin96a] [Sabourin97].

Consequently, research in the rapid prototyping industry is focused on enhancing part accuracy and reducing fabrication time simultaneously. One technique that has originated from these efforts is adaptive slicing, which minimizes the stair-stepping inaccuracies by adapting the thickness of each build layer to better match the part surface geometry. Several methods have been introduced which survey the surface geometry at each layer to determine an appropriate thickness for that layer. With these methods, vertical and near-vertical surfaces are built with relatively thick layers, while flat and near-flat surfaces are built with thinner layers. Hence, the layer resolution is increased where the geometry would tend to produce more significant errors due to stair-stepping.

However, conventional adaptive slicing routines are limited in that they are one-dimensional, only varying the build layer thicknesses with a change in vertical position (height). As a consequence, these methods are ill suited for an industrial setting in which the build envelope is typically filled with parts and part features at the same horizontal levels having vastly dissimilar surface characteristics. In such situations, too many of these parts and features are fabricated with needlessly thin layers only to satisfy the needs of some remote part or feature elsewhere in the build envelope at that particular height (Figure 1.2).

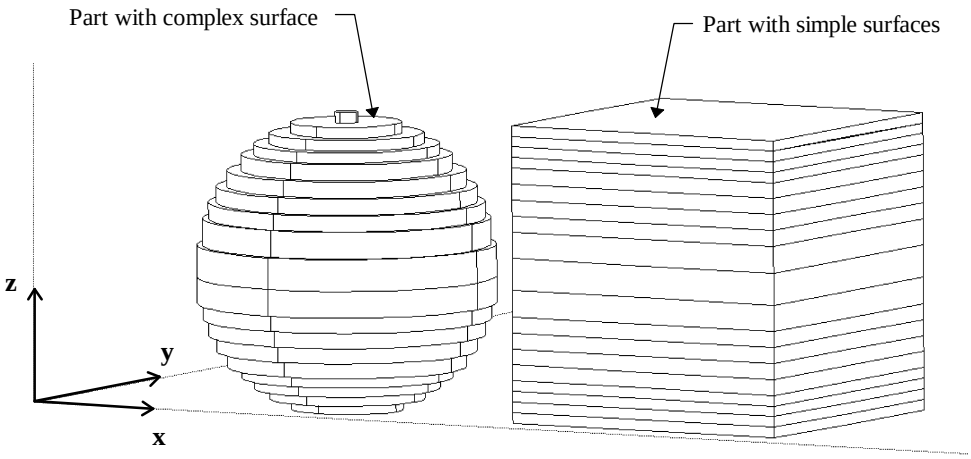

Figure 1.2: The potential savings of adaptive slicing is lost by conventional adaptive slicing methods, which slice all parts of a given build with the same resolution, regardless of their dissimilar surface characteristics. This results in unnecessary build layers for the simpler geometries. In the case shown here, the thin layers necessary for the sphere are imposed unnecessarily on the block.

Furthermore, the literature addressing these conventional adaptive slicing methods has thus far been limited to the theoretical control of build layer thicknesses. Indeed, adaptive slicing has not been implemented on commercial layered manufacturing systems primarily because fabrication with adaptive build layer thicknesses is not well supported. For example, reducing adaptive slicing to practice using a FDM 1600 rapid prototyping system often produces surface discontinuities that are particularly apparent when transitioning from one layer thickness to another. Hence, using this system to fabricate adaptively sliced parts requires that it be calibrated for multiple build layer thicknesses simultaneously.

1.1 PROBLEM STATEMENT AND OBJECTIVES

Conventional adaptive slicing routines slice all parts of a given build with the same resolution, regardless of their dissimilar surface characteristics. Consequently, these methods are unable to realize the full potential of adaptive slicing (to reduce fabrication times) due to the fabrication of unnecessary build layers. Furthermore, commercial layered manufacturing systems do not support fabrication with adaptive build layer thicknesses.

Therefore, this thesis has two objectives. The first objective is to develop a new approach to adaptive slicing that applies adaptive slicing techniques locally across part geometries such that individual parts and part features are fabricated independently of one another with respect to build layer thicknesses. This new approach will effectively eliminate unnecessary build layers and thereby minimize fabrication times. The second objective is to reduce adaptive slicing to practice by fabricating high quality, adaptively sliced parts using a FDM rapid prototyping system. In particular, this objective involves the calibration of adaptive build layer thicknesses relative to one another to reduce surface discontinuities at transitions between build layers with dissimilar thicknesses.

1.2 SOLUTION OUTLINE

The simplest, most widely practiced slicing method employed by the LM industry produces horizontal layers of equal thickness throughout the CAD model. This is called uniform slicing. With uniform slicing, details of the geometric data supplied by the CAD model are often ignored. Minor changes in geometry of the model surfaces are frequently not accounted for [Dolenc94], and inaccuracies like those illustrated in Figure 1.3 are introduced. Adaptive slicing methods improve the overall part accuracy by adjusting the build layer thicknesses to accommodate surface geometry.

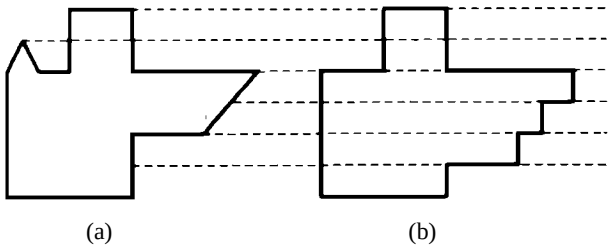

Figure 1.3: The effects of uniform slicing. (a) Original model; (b) fabricated part; [Dolenc94].

This thesis presents a new adaptive slicing method that minimizes the fabrication time required when employing adaptive slicing principles by slicing and fabricating each part and individual part feature independently of one another within the build envelope. This new method ensures that thin build layers are used only where necessary and thicker build layers are used elsewhere (Figure 1.4).

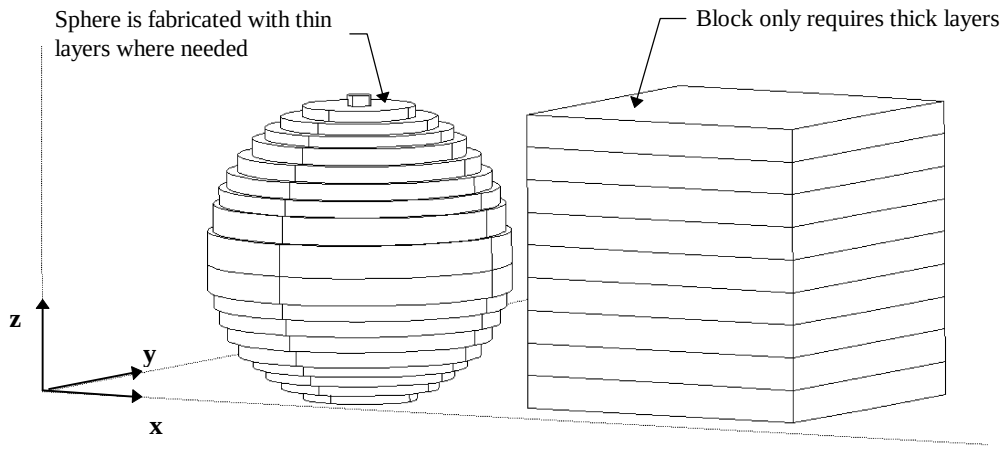

Figure 1.4: Individual parts are fabricated independently with distinct layer resolutions applied locally as necessary.

To accomplish this task, the model is first sliced into thick slabs with the maximum thickness allowed by the fabricator. The resulting contours belonging to a slab's top and bottom slices are then matched using topological information to form a set of sub-slabs (Figure 1.5). Finally, adaptive slicing is performed by sub-dividing each thick sub-slab into a distinct number of thinner layers based on the vertical slope of its surface, measured along the contours that define it.

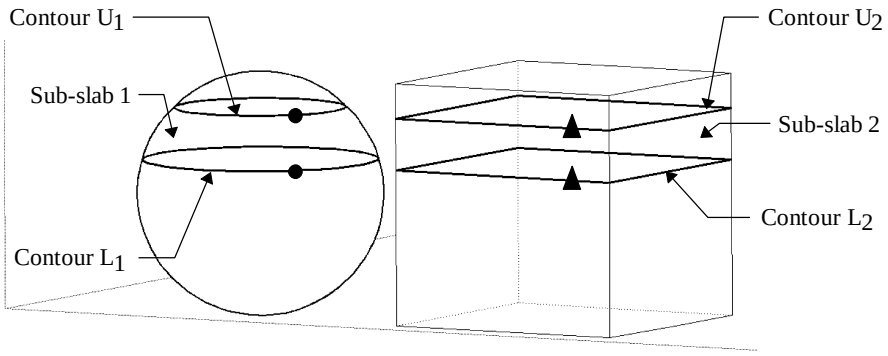

Figure 1.5: Lower contours L_1 and L_2 are matched with upper contours U_1 and U_2 to form sub-slabs 1 and 2 respectively. Sub-slab 1 can then be divided into *m* thinner layers, while sub-slab 2 is divided into *n* layers, with $m > n$.

The advantage of implementing this new approach to local adaptive slicing over conventional adaptive slicing and uniform slicing methods is controversial at best if the parts fabricated with the new approach exhibit poor surface quality. Therefore, a calibration method for a FDM rapid prototyping system that enables robust fabrication with adaptive build layer thicknesses is provided. In particular, the specific build parameters that are associated with this system and contribute to surface discontinuities are identified. Then, a simple procedure to ensure that the system is calibrated for use with multiple build layer thicknesses is detailed. Finally, observations made from experimental builds are used to recommend specific build parameter values that will support robust fabrication with this system.

1.3 THESIS ORGANIZATION

The remainder of this thesis details the new approach to local adaptive slicing as well as the calibration procedure that enables fabrication with adaptive build layer thicknesses using the FDM rapid prototyping system. It consists of the following:

Chapter 2 provides background material that is necessary to obtain a better understanding of layered manufacturing as it pertains to this thesis. It also presents a survey of recent work that has been done in the field of layered manufacturing. Specifically, methods to improve slicing efficiency and surface smoothness are addressed.

Chapter 3 details the methodology of the new approach to local adaptive slicing, which is used to minimize the occurrence of unnecessarily thin build layers, thereby minimizing fabrication times.

Chapter 4 outlines the new calibration procedure that has been successfully implemented for the FDM rapid prototyping system.

Chapter 5 presents concluding remarks, outlines contributions, and gives recommendations for future work.

CHAPTER 2

LITERATURE REVIEW

Layered manufacturing (LM) technologies have secured a position in modern design processes by enabling fast and frequent design iterations. Designers are able to produce prototype parts that assist them in eliminating potential design flaws early in a product's development cycle. However, a major limitation of LM systems is their inability to achieve acceptable part surface quality within an acceptable amount of time. To overcome this limitation, ongoing research is exploring advances in software, hardware and materials. This chapter provides important background information related to LM processes and the methods presented in this thesis. It then reviews current research, focusing on efficient CAD model processing, efficient software controlled fabrication strategies, and advanced hardware solutions.

2.1 TOPOLOGY, DEFINITIONS, AND CONVENTIONS

This section presents a definition of topology as it is used in the context of this thesis. It also provides brief definitions that are used throughout this thesis to describe entities that are commonly associated with LM processes. These definitions are not generic, but merely describe how this thesis refers to each entity. Finally, this section details the contour orientation convention as it applies to the LM industry.

2.1.1 Use of Topology

One aspect of topology is the connectivity information that relates the components of a composite entity. In particular, each component may be related to its sub-components, or the components that contain it as a sub-component. In addition, a component may also be related to its neighboring components. In this thesis, the composite entity of interest is a solid described in the .STL file format. This format describes the boundary representation of 3D geometry with a series

of interconnected triangular facets that are defined by three edges. Each edge, in turn, is defined by two vertices. Therefore, the term topology in this thesis will refer to the information that describes the connectivity between each facet, edge and vertex that comprise the surface of a solid. Specifically, this thesis assumes that each facet at minimum includes references to its three edges, as well as its neighboring facets; and that each edge contains references to its two vertices.

2.1.2 Brief Definitions

Vertex A vertex is a zero-dimensional topological entity. Its geometric representation is a point, which in 3D space is described with three spatial coordinates.

Edge An edge is a one-dimensional topological entity that connects two vertices. An edge typically has a direction. In this case, one of its vertices is denoted its head, and the other, its tail. In this thesis, the term edge will also be used to denote a linear line segment in 3D space.

Facet A facet is a planar geometric entity. In this thesis, the term facet will be used to denote a triangular planar entity that is defined by an ordered list of three edges. These edges are implied by an ordered list of three vertices. A facet has a directed normal that is perpendicular to the facet plane, and is oriented according to the "right hand rule" applied to the ordered list of vertices.

Solid A solid is a collection of interconnected facets. They must form a closed, oriented, and topologically two-manifold shell. This implies that its facet normals must all be directed away from the material.

Feature A feature is a partial volume of a solid. It is a unique geometric entity that emanates from a solid, such as a protrusion.

Slice A slice is a two-dimensional plane that describes a horizontal cross section of a solid.

Contour The term contour in this thesis denotes a two-dimensional entity comprised of a collection of directed edges. It bounds the material regions of a given slice. It is closed and oriented.

Layer A layer is a partial volume of a solid. It represents the material bounded by two adjacent slices.

Slab A slab is a thick layer corresponding to the maximum layer thickness with which a particular LM system is capable of fabricating.

Sub-slab A sub-slab is defined by two or more contours from the slices that bound a slab. The contours must be derived from the same feature. This can be established using topological information.

2.1.3 Contour Orientation Convention

On a given slice, the material regions are circumscribed by a set of contours. By convention, these contours are directed such that the material lies to the left of the contours, as viewed in the direction of the contour. Therefore, external contours are directed counterclockwise (CCW), and internal contours are directed clockwise (CW). This is illustrated in Figure 2.1.

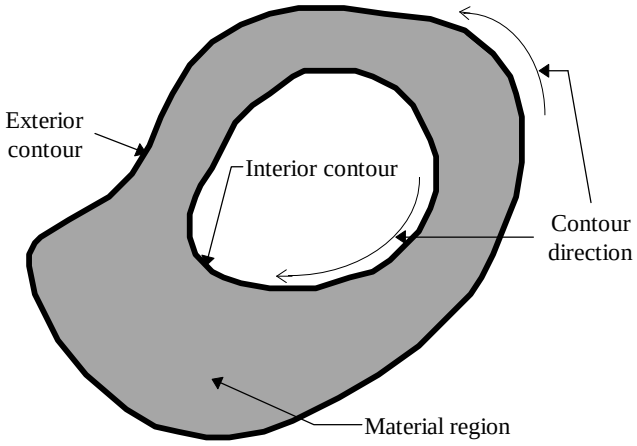

Figure 2.1: Contour orientation convention. Interior contours are directed clockwise, while exterior contours are directed counterclockwise.

2.2 FILE FORMATS

All current commercial LM systems require that the geometry to be fabricated be described in the .STL file format. Once in this format, the geometry is sliced to obtain the horizontal cross-sections. These cross-sections are then used to generate the NC toolpaths required by the fabricator.

2.2.1 .STL

The .STL file format [Burns93] consists of an unordered list of triangular facets that approximate the actual surfaces of an original CAD model. It is a boundary representation of 3D geometry. Figure 2.2 illustrates a faceted representation of a sphere.

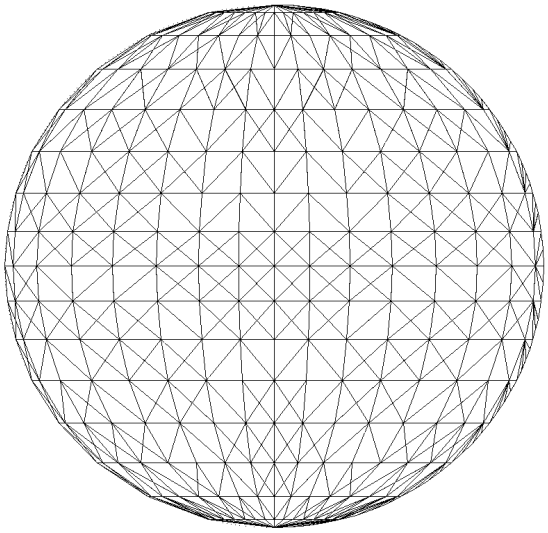

Figure 2.2: Faceted representation of a sphere.

The .STL file format has become the *de facto* industry standard for describing CAD models to LM processes for two reasons. First, 3D Systems, Inc. introduced the format three years prior to any other for use with their Stereolithography Apparatus (SLA). Second, its extremely simplistic format for describing CAD models minimizes the cost of providing one-way translation. As a

result, most CAD vendors have developed software that is capable of translating data to this format.

However, the .STL file format contains minimal topological information. Specifically, it contains a list of possibly unconnected triangular facets. Hence, there is no guarantee that a .STL model is closed and properly oriented. A model that is not closed and properly oriented cannot be fabricated because it does not describe a rigid solid. Therefore, it must first be repaired before it can be sliced. Furthermore, without topology, it is much more difficult to check a faceted model for closure and orientation before the slicing process is implemented.

The lack of topological information in the .STL file format is also a source of unnecessarily large files containing redundant and possibly inconsistent data. In the .STL file format, each facet is represented by three vertices whose coordinates are explicitly described. This causes considerable redundancy since each vertex is described once each time it is used, which is at a minimum three times, and often ten times or more. The .STL format also explicitly describes the surface normal for each facet, in addition to defining it implicitly by the order of the facet's vertices using the right hand rule. These duplications are sources of inflated file sizes and possible inconsistencies.

2.2.2 Other File Formats

As a result of the deficiencies of the .STL file format, Rock and Wozny [Rock91a] developed a new file format that makes use of indexed lists to represent vertices, edges and facets in a manner similar to that of the IGES file format [USPro96]. In this file format, each facet references the appropriate vertices via indices into a vertex list instead of storing nine explicit entries corresponding to the three vertices' 3D coordinates. This establishes topological information, eliminates redundant vertex definitions, reduces the likelihood of inconsistencies, and significantly reduces the required file size.

The new file format is called the .RPI file format, and it can be derived from the .STL file format at some computational cost. Specifically, the cost emerges from inferring topology using the topology reconstruction algorithm outlined in [Rock92]. This algorithm incorporates three

sequential stages: vertex merging, edge and facet creation, and the determination of the relationships between these edges and facets. Upon completion of the last stage, each facet references its three edges as well as its neighboring facets. Each edge, in turn, references its two vertices and the two facets that define it.

Several other file formats have been developed for use with LM technologies. The Standard Triangles Hinted (.STH) file format also employs indexed lists to describe a 3D model which may be comprised of ruled surfaces, polygons, bounded planes, or a collection of triangular facets [Brock91]. The Common Layer Interface (.CLI) file format describes the cross-sectional data of a model using polygonal contours [CLI98]. This file format originated primarily from the need to describe computed tomography (CT) scan data to LM technologies being used in the medical industry. The .CLI format is also used by some to store the cross-sectional data obtained from slicing models directly with CAD software [Jamieson95] [Krause97]. The Layered File Format (.LFF) is being developed by Zheng and Newman for use with their CAM-LEM process [Zheng97]. This format is also used with direct CAD model slicing, and supports edges, polylines, elliptic arcs and B-splines. Finally, the Virtual Reality Modeling Language (VRML) format can be used in a virtual environment that allows users to manipulate vertices to modify triangles [Fadel96].

2.3 EFFICIENT SLICING

The lack of topological information in the .STL file format makes model slicing expensive since each facet must first be checked to determine if it intersects a given slice plane, and then all the edges obtained from these intersections must be sorted to form closed contours. To overcome this problem, Rock and Wozny [Rock91b] developed a method that greatly enhances the speed and efficiency with which a given model is sliced. This method, known as the marching algorithm for slicing, makes use of topological information while intersecting the facets with slice planes. Their algorithm eliminates the requirement to sort the edges obtained by intersecting facets with slice planes in the contour generation process. Instead, contours are ordered as they are

constructed by 'marching' from facet to neighboring facet. The result is a faster, more efficient slicing procedure.

Rock and Wozny observed that each intersecting facet has two intersecting edges, as shown in Figure 2.3. The intersection of these two edges defines a contour edge. The adjacent contour edges, in turn, are defined by the intersection of the two adjacent intersecting facets. Adding topology enables each facet to reference the facets that share its edges. With this connectivity known, an ordered contour can be constructed by 'marching' from facet to neighboring facet given an initial facet that intersects the slice plane. Hence, the requirement to sort the edges obtained by intersecting the facets with a given slice plane is eliminated.

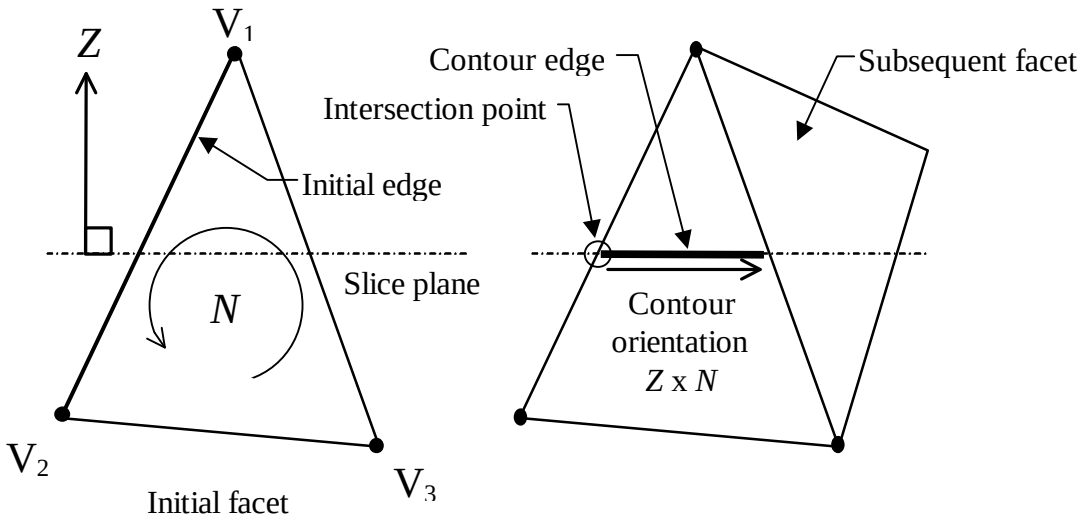

Figure 2.3: A facet that intersects the slice plane has two intersecting edges. Once the intersection of the initial edge is found, the marching direction is determined by *Z* x *N*.

Once the intersection of the initial facet edge is performed, the direction of the march must be established to properly define the orientation of each contour. This direction is given by $Z \times N$, where Z is the vertical vector and N is the facet's surface normal. Rock and Wozny [Rock91b] deduce this direction by determining the relative position, with respect to the slice plane, of the facet vertex that lies opposite the initial edge. For instance, in Figure 2.4, if edge E_{12} of facet $F_A(V_1, V_2, V_3)$ is the initial edge, with vertex V_1 lying above the slice plane and vertex V_2 below

it, then the next edge to be intersected will be E_{13} if vertex V_3 lies below the plane, or E_{23} if V_3 lies above the plane. The corresponding adjacent facets would be F_{13} and F_{23}, respectively. The algorithm continues traversing subsequent facets until the initial edge is reached, at which point the contour is complete.

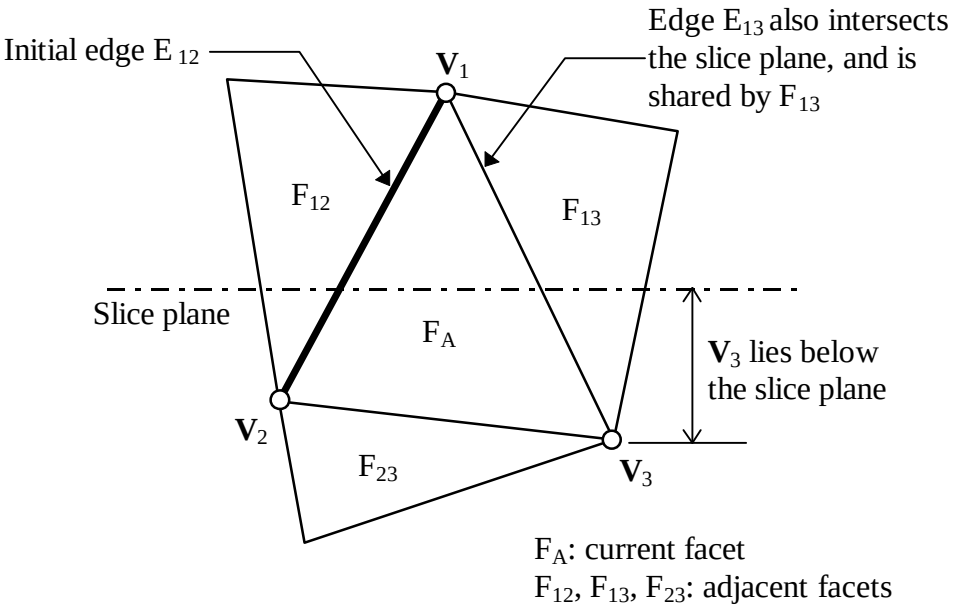

Figure 2.4: Given an initial facet F_A with intersecting edge E_{12}, the next intersecting edge is determined by the relative position of the vertex V_3. In this case, since V_3 is below the slice plane, the next edge to be intersected is E_{13}. The corresponding facet F_{13} is then used to determine the ensuing edge.

The extensive number of edge/plane intersections in the overall slicing process requires that the calculation used to obtain these intersections be fast and efficient. Recognizing this, Rock and Wozny [Rock91b] developed the following procedure for obtaining the intersection of an edge and a plane. This method has been optimized such that the computational expense, in particular, the number of floating point operations (FLOPS) is minimum.

The planes used to slice a solid are horizontal. Therefore, each plane can be represented, in the Cartesian coordinate system in Euclidian 3-space, by the equation

$$z = h \tag{2.1}$$

where *h* is the height of the plane. In addition, an edge defined by two vertices $\mathbf{p} = (x_p, y_p, z_p)$ and $\mathbf{q} = (x_q, y_q, z_q)$ can be described in parametric form by

$$\mathbf{P}(t) = \mathbf{p} + t\,(\mathbf{q} - \mathbf{p}) \tag{2.2}$$

with $t \in [0,1]$. Rock and Wozny show that if one of these points lies above the slice plane, and the other lies below it, then the edge/plane intersection resides at

$$t = \frac{h - z_p}{z_q - z_p} \tag{2.3}$$

Assuming one FLOP for each addition, subtraction, and multiplication, and five FLOPS for each division [Bøhn89], *t* can be computed in seven FLOPS. The *x* and *y* coordinates of the intersection point can then be computed in an additional six FLOPS using equation (2.2). Hence, the total number of FLOPS required for the entire calculation is 13 FLOPS.

Rather than address the problems directly associated with the .STL file format, Kirschman and Alamonte [Kirschman92] proposed parallel processing as a means to reduce slice times. They implemented a parallel slicing algorithm in which 2,4,8,16 and 32 concurrent processors were used to carry out the slicing procedure. Theoretically, fabrication times can be reduced by 93.75% and 96.875% when using 16 and 32 processors, respectively, as compared to a single processor implementation.

2.4 DIRECT CAD MODEL SLICING

Direct CAD model slicing originated from the desire to provide LM fabricators with a CAD model description that was more accurate than that provided by the .STL file format. A model description in the .STL file format can only approximate the curved surfaces of a CAD model from which the .STL file is derived. Furthermore, the cross-sections resulting from slicing tessellated models are comprised of polygonal contours that can only approximate the true cross-sections of higher order surfaces such as spheres or Non-Uniform Rational B-splines (NURBS). In addition, the translation of CAD models to the .STL file format often produces errors such as missing and intersecting facets, and repairing these models is an expensive and imperfect task.

One approach to resolve these issues is to slice the CAD model directly. The primary benefits of direct CAD model slicing are increased model accuracy and smaller file sizes. Researchers contend that, by slicing the model within the CAD software, exact contours can be derived from the model's true surfaces [Guduri92] [Zheng97]. In addition, storing the cross-sectional data requires less space than a tessellated model would require [Vuyyuru94] [Jamieson95] [Beaman97]. Also, the need for model repair and a conventional slicing process is eliminated.

As a result, many research groups have implemented direct CAD model slicing. Guduri *et al.* [Guduri92] developed an interface to LM processes based on constructive solid geometry (CSG). In their work, a part to be fabricated is represented by CSG primitives. Each primitive is sliced individually to generate a set of independent contours. Boolean operations are then performed at the intersections of these contours to produce each slice. Hope *et al.* [Hope97a] [Hope97b] also developed their own CAD model slicing software, TruSurf, which makes use of the IGES file format [USPro96] (supported by most commercial CAD systems) to translate CAD models. Several research groups have also made use of existing commercial CAD systems to perform model slicing. Vuyyuru *et al.* [Vuyyuru94] sliced a solid model using SDRC's I-DEAS CAD package to obtain contours represented by NURBS. Jamieson and Hacker [Jamieson95] used Parasolid, the solid modeling kernel provided by EDS Unigraphics, to output slice curves in the .CLI file format [CLI98], and Zheng and Newman [Zheng97] utilize ACIS, the 3D geometric modeler from Spatial Technology, to produce slice data described in their .LFF file format.

Despite the benefits of direct CAD model slicing, commercial LM systems continue to primarily support the .STL file format for several reasons. The main advantage of the .STL description is the simplicity of the intersection calculations (detailed in the previous Section) required for slicing [Beaman97]. Slicing high-degree polynomial surfaces (NURBS), on the other hand, is non-trivial [Guduri92] and prone to round-off errors [Beaman97]. Furthermore, there is currently no standard higher-order geometric description available to exchange geometric data from a particular CAD system to a specified LM fabricator.

2.5 ADAPTIVE SLICING

The most significant development in LM technology, in terms of improved part accuracy, has been adaptive slicing. The basic principle of adaptive slicing is to evaluate local surface geometries to determine the maximum build layer thickness that can be used while maintaining a user-defined surface tolerance, usually measured by the cusp height. The cusp height represents the maximum deviation of the part surface from the true surface. As shown in Figure 2.5, it is measured in the direction normal to the true surface. The layer thicknesses are usually distinct values bound by [L_{min}, L_{max}] which are pre-determined by the user and which are limited by the fabrication capabilities of the specific LM process. Existing methods typically incorporate mathematical expressions that predict the cusp height at discrete locations along a given slice. These expressions are then used to determine the optimal thickness for each layer based on the part surface curvature. Dolenc and Mäkelä [Dolenc94], Suh and Wozny [Suh94], Kulkarni and Dutta [Kulkarni95] [Kulkarni96], Sabourin *et al.* [Sabourin96a] [Sabourin96b] [Sabourin97], and Krause *et al.* [Krause97] have all developed methods that employ these techniques.

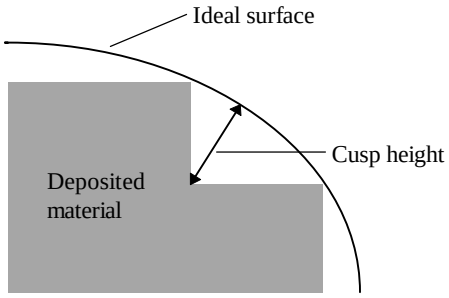

Figure 2.5: The maximum deviation between the ideal surface and the surface of the fabricated part is given by the cusp height. The cusp height is measured in the direction normal to the ideal surface.

Dolenc and Mäkelä [Dolenc94] demonstrate the important advantage of using adaptive slicing techniques rather than uniform slicing. Figure 2.6 [Dolenc94] illustrates the possible effects of fabricating a part that has been uniformly sliced. When using this method, flat areas and peak features of a part may not be accounted for. However, with adaptive slicing, it is possible to place

slice heights at locations that coincide with these key features, thereby eliminating significant errors.

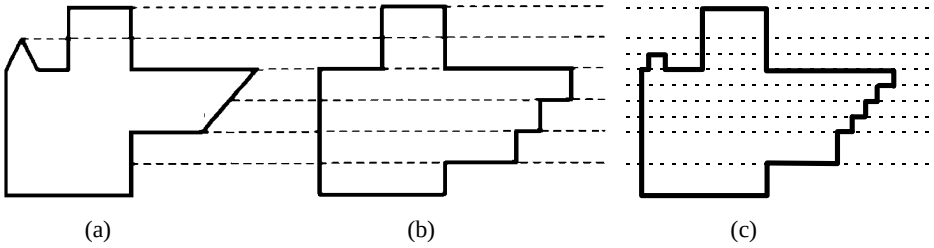

Figure 2.6: The effects of uniform slicing. (a) Original model; (b) uniformly sliced part; (b) adaptively sliced part; [Dolenc94].

In addressing the stair-stepping problem, Dolenc and Mäkelä focus on polyhedral models such as those described in the .STL file format. They observe that the layer thickness required to satisfy the specified surface tolerance, C_{max}, in the vicinity of a point P on the part surface is dependent upon n_z, the vertical component of $\bar{n}$ which is the unit surface normal at P. Specifically, they observe that the cusp height c is maintained below C_{max} if $\bar{C} = c\bar{n}$ satisfies $\|\bar{C}\| = c \le C_{max}$ (Figure 2.7).

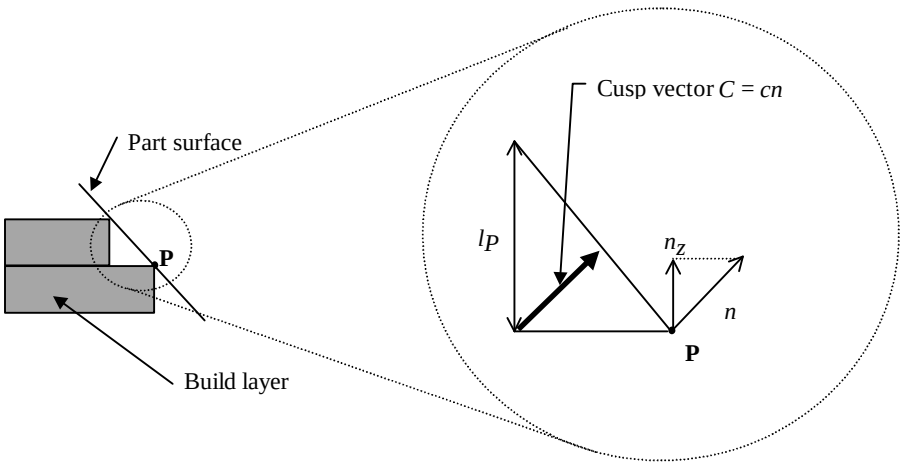

Figure 2.7: Determining the build layer thickness from the cusp vector C, and the vertical component of the unit normal to the surface; [Dolenc94].

Given C_{max}, the optimal layer thickness at P is therefore

$$l_P = \min\{L_{max}, C_{max} / n_z\} \tag{2.4}$$

A layer thickness is determined for several discrete points P_i along a given slice and the minimum is used to fabricate the layer above it, provided that it is larger than the minimum thickness available:

$$l_{slice} = \max\{L_{min}, \min\{l_{P_i}\}\} \tag{2.5}$$

Suh and Wozny [Suh94] divide each model into sub-regions whose vertical boundaries are defined by the model's peak features. With the peak features accounted for, each sub-region is then adaptively sliced. The thickness of each layer, d, is calculated by first sampling the surface geometry at several points along the previous slice. The minimum of these calculated values is then considered the optimal layer thickness. Suh and Wozny determine the thickness at a sample point P by approximating the part surface geometry using a sphere of radius r, based on the part surface curvature at that point. The thickness is then computed from equations that are derived from the geometry shown in Figure 2.8 for points on upward and downward facing surfaces, respectively.

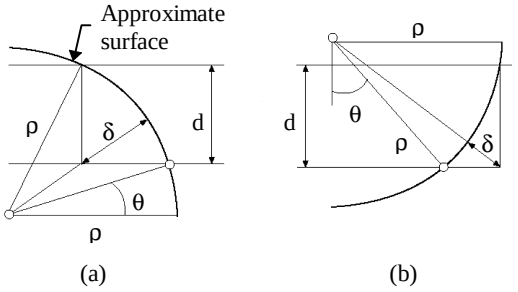

Figure 2.8: Approximation of the local surface curvature with a sphere to obtain an appropriate build layer thickness *d*; [Suh94].

The sampling points, P_i, along each slice are determined by approximating the contour curves by arcs, as shown in Figure 2.9. From a given sampling point, the location of the next sampling point is calculated from equation (2.6).

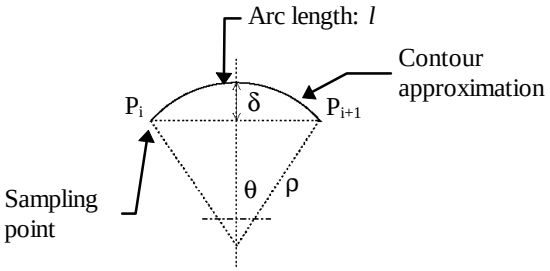

Figure 2.9: Determining the location of sampling points along a given contour. From a sampling point P_i, the location of the next sampling point P_{i+1} is dependent upon the radius of curvature of the contour r and the cusp height d; [Suh94].

$$\text{arc length } l = \begin{cases} \infty & \text{if } r = 0 \\ 2r\cos^{-1}(1-\frac{d}{r}) & \text{otherwise} \end{cases} \tag{2.6}$$

Kulkarni and Dutta [Kulkarni95] [Kulkarni96] correct and expand upon the method developed by Suh and Wozny by identifying all possible configurations that could arise during the calculation of a given build layer thickness (Figure 2.10). While Suh and Wozny only differentiate between upward and downward facing surfaces in their calculations, Kulkarni and Dutta also consider the differences in curvature for both of these situations. As a result, they recognized four unique configurations (Figure 2.10) as opposed to just the two identified by Suh and Wozny, and derived expressions for each to determine the curvature at a given point. Equations 2.7, 2.8, 2.9 and 2.10 correspond to the cases shown in Figures 2.10a-d, respectively. Their derivations are shown in Appendix A.

$$d = -r\sin q + \sqrt{r^2\sin^2 q + 2rd - d^2} \tag{2.7}$$

$$d = -r\sin q + \sqrt{r^2\sin^2 q + 2rd + d^2} \tag{2.8}$$

$$d = r\sin q - \sqrt{r^2\sin^2 q - 2rd + d^2} \tag{2.9}$$

$$d = r\sin q - \sqrt{r^2\sin^2 q - 2rd - d^2} \tag{2.10}$$

Furthermore, Kulkarni and Dutta limit their geometry to parametric surfaces represented by algebraic equations. They are therefore able to extract the exact expression for the surface curvature in the vertical direction along each slice level. The curvatures computed by Suh and Wozny, on the other hand, contain a level of uncertainty because each is obtained by sampling discrete points along each level.

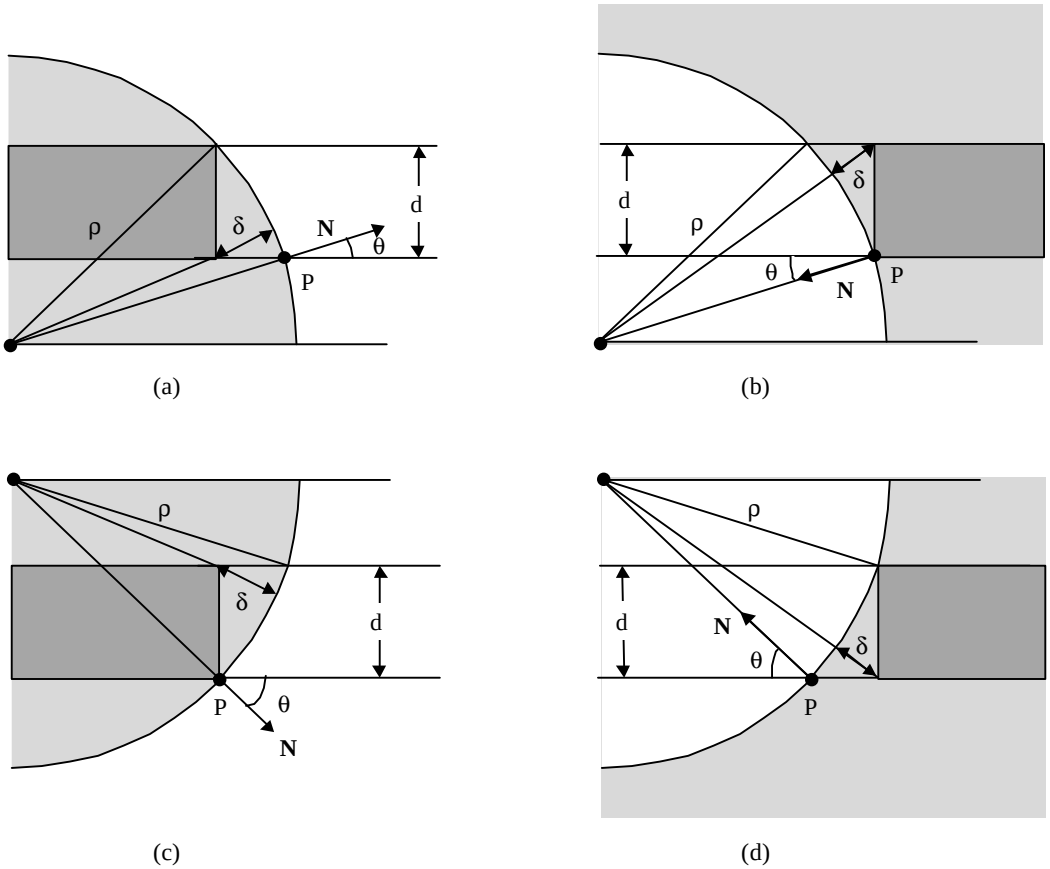

P: a point on the part surface

N: the surface normal at P

θ: the angle that **N** makes to the horizontal

ρ: the radius of curvature at P

δ: the allowed cusp height

d: the layer thickness to be computed

Figure 2.10: Four possible configurations that may be encountered when using the build layer thickness approximation method developed by Kulkarni and Dutta; (a) convex curvature on upper hemisphere; (b) concave curvature on upper hemisphere; (c) convex curvature on lower hemisphere; and (d) concave curvature on lower hemisphere; [Kulkarni96]

The methods introduced by Suh and Wozny [Suh94] and Kulkarni and Dutta [Kulkarni95] [Kulkarni96] were developed using non-polyhedral surface representations. As a consequence, neither method is suitable for faceted models such as those described in the .STL file format.

Sabourin *et al.* [Sabourin96a] [Sabourin96b] offer an alternative approach to adaptive slicing that does apply to the .STL file format. In what they term *stepwise uniform refinement*, each model is first sliced into thick, uniform, horizontal slabs. Each slab has a thickness corresponding to the maximum layer thickness that can be fabricated. These slabs are then uniformly sub-divided individually, as needed, to satisfy the cusp height requirement developed by Dolenc and Mäkelä [Dolenc94]. However, unlike the previous methods, this method applies the measure $l_P = C_{\max} / n_z$ to both the top and bottom slices that define each slab rather than to the bottom slice only. Furthermore, Sabourin *et al.* perform adaptive slicing by determining the optimal integer number of uniform thickness slice layers that a particular slab is to be subdivided into:

$$a_{slab} = \operatorname{int}\left(\frac{L_{\max}}{C_{\max}} \max\{ n_{z_{top}}, n_{z_{bottom}} \} \right)$$
$$a_{slab} \in [1, a_{\max}], \quad a_{\max} = \operatorname{int}\left(\frac{L_{\max}}{L_{\min}} \right) \tag{2.11}$$

where $\{n_{z_{top}}\}$ and $\{n_{z_{bottom}}\}$ are the sets of unit normal z components for the points P_i along the top and bottom slices of a particular slab, respectively. This ensures that every point P along the pair of slices is considered in the calculation of the optimal layer thickness within that slab. This thickness is then given by

$$l = L_{max} / a_{slab} \tag{2.12}$$

By evaluating the surface characteristics at every point along both the top and bottom slice levels, this method is less likely to miss regions of extreme curvature during the slicing process [Sabourin96a] [Sabourin96b].

Suh and Wozny [Suh94], Kulkarni and Dutta [Kulkarni95] [Kulkarni96], and Sabourin *et al.* [Sabourin96a] [Sabourin96b] each report an increase in fabrication speed when comparing parts sliced using their respective methods with the identical uniformly sliced parts. Each group attributes this speedup to the lesser number of layers required to produce an adaptively sliced part. Suh and Wozny [Suh94] generated a 10 inch (254 mm) diameter sphere using both uniform and adaptive slicing techniques. The adaptively sliced version required 909 layers that ranged in thickness from 0.001 inch (0.03 mm) to 0.020 inches (0.51 mm). A layer thickness of 0.006 inches (0.15 mm) was used for the uniformly sliced version, which required 1667 layers. The cusp height was maintained below 0.006 inches (0.15 mm) in both cases. Kulkarni and Dutta [Kulkarni95] [Kulkarni96] reported an 18 per cent reduction in fabrication time when comparing an ellipsoid that was adaptively sliced to a uniformly sliced version. The former required just 82 layers, while 146 were required for the uniformly sliced model. Finally, Sabourin *et al.* [Sabourin96a] [Sabourin96b] built a part using uniform 0.005 inch (0.13 mm) thick layers, and then again with adaptive slicing using discrete layer thicknesses of 0.0050, 0.0075 and 0.0150 inches (0.13, 0.19 and 0.38 mm) as needed. The result was a 52 per cent reduction in measured build time, while going from 79 to 41 layers.

In an effort to further reduce build times, Sabourin *et al.* [Sabourin96a] [Sabourin97] developed a unique method that combines the use of thick and thin build layers. The approach involves separating the model space into interior and exterior regions as illustrated in Figure 2.11 [Sabourin96a] [Sabourin97]. After slicing the model space into thick slabs [Sabourin96b], they offset the external contours of the subsequent slices into the model (Figure 2.12) [Sabourin96a] [Sabourin97]. The offset curves mark the boundary between the interior and exterior regions. The latter are then re-sliced using stepwise uniform refinement [Sabourin96b] to enhance the quality of the part surfaces, while the interior regions are built with thick layers to increase the fabrication speed. By increasing the throughput of the material deposition in the interior regions, they were able to realize an additional approximate 50 per cent reduction in fabrication times [Sabourin96a] [Sabourin97].

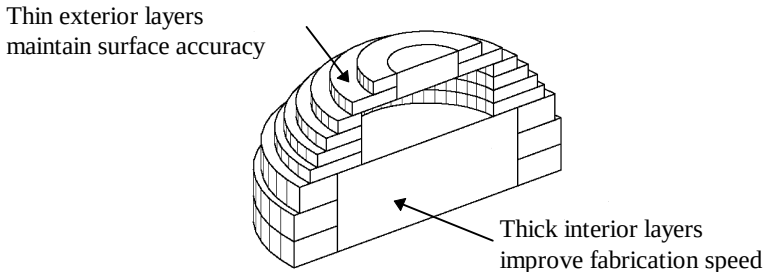

Figure 2.11: The overall fabrication time is reduced by increasing the throughput of material deposition of the thick interior layers while the surface quality is maintained with thin exterior layers; [Sabourin96a] [Sabourin97]

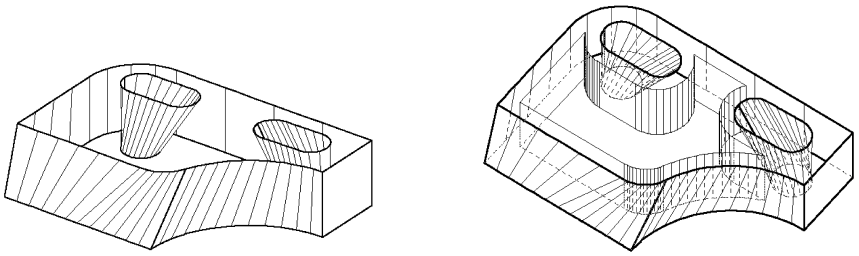

Figure 2.12: An example of interior and exterior segregation due to contour offsetting. (a) A thick slice; (b) the same slice segregated into interior and exterior regions; [Sabourin96a] [Sabourin97]

All of the above adaptive slicing procedures determine a given build layer thickness by evaluating the surface curvature along the slice levels that define it. With these methods, the minimum build layer thickness computed along each slice level is used to fabricate all parts and individual part features existing at that height across the build envelope. This produces unnecessary build layers whenever any of these parts or features do not require this minimum layer thickness to meet the overall surface tolerance. The result is a needlessly inefficient build process.

Recognizing this flaw, Krause *et al.* [Krause97] have introduced an approach that uses a feature recognition algorithm to divide each CAD model into a set of arbitrary partial volumes, or segments, based on their unique geometries. Each segment of the part is then sliced

independently according to its own surface characteristics. This new method elicits the full potential of adaptive slicing processes, enabling separate part features that exist at a given height to be fabricated independently with distinct build layer thicknesses as needed. This is similar, conceptually, to the method presented in this thesis, though the implementation of each differs substantially.

Krause *et al.* make use of the ACIS solid modeling kernel from Spatial Technology to process their CAD models. This enables them to separate each model into partial volumes. The surfaces of each of these segments are then analyzed to determine the segment's layer resolution. Although the specifics of their feature recognition algorithm are not described in [Krause97], it is likely that this algorithm will have difficulty processing intricate parts containing randomly located features with highly convoluted surfaces.

The method presented in this thesis relies on the .STL file format and the techniques described in [Dolenc94] [Sabourin96a] [Sabourin96b] [Sabourin97]. Specifically, it first slices the CAD model into thick slabs using the maximum layer thickness available. Then it pairs contours on adjacent slices to establish independent sub-slabs. These sub-slabs can then be independently sliced adaptively using stepwise uniform refinement.

2.6 SLOPED LAYERS

The previous adaptive slicing techniques all make use of 2½D layers in fabricating models for LM processes. These procedures simply extend the contours of the 2D slice levels in the (vertical) build direction to obtain the thickness of each build layer. A repercussion of this methodology is the stair-stepping effect, which can only be reduced by using thinner layers and, consequently, increasing the fabrication time.

An alternative approach is to employ LM systems that can fabricate with sloped layers. The principal advantage of this approach is that adjacent slices are ensured C^0 continuity at the part surface, thereby significantly reducing the errors produced by stair-stepping (Figure 2.13). A number of sloped-layer fabrication systems have been developed. Several of these systems [Thomas96] [de Jager97] [Hope97a] [Hope97b] [Zheng97] cut out sheets of material, machine

their vertical surfaces to achieve the sloped shape, and stack them using a sintering [Zheng97] or gluing process [Hope97a]. The Shape Deposition Manufacturing (SDM) process, on the other hand, deposits droplets of molten metal to achieve each layer, and machines the surfaces afterwards using a 3 or 5-axis mill [Merz94] [Klingbeil97].

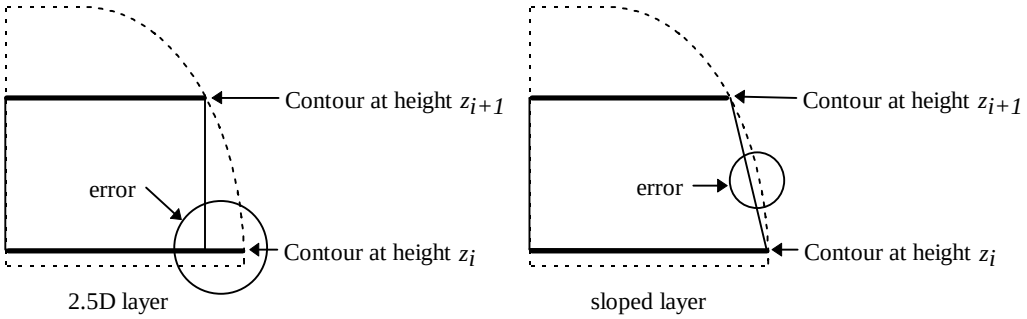

Figure 2.13: Comparison of errors produced by 2½D and sloped (ruled) layers; [de Jager97].

As with 2½D layers, the creation of each sloped layer requires the establishment of the contours that define it. However, sloped layers that are machined require further computations to produce an approximate surface between these two contours, and an accurate cutting vector along this surface. The process of establishing an approximate surface between two contours is not new. Keppel [Keppel75] joined points along neighboring contours to form a surface that was approximated by triangular planar elements. Most current researchers simplify this by approximating the layer surfaces with ruled surfaces [Thomas96] [de Jager97] [Zheng97]. These are obtained by connecting points along adjacent contours with a series of straight-line segments.

Both de Jager *et al.* [de Jager97] and Zheng and Newman [Zheng97] perform direct CAD model slicing to obtain the slice contours. They use ruled surfaces to define the outer surface of each layer. This enables tangent-cutting of each layer by at least a four axis system that employs line visibility [de Jager97] [Zheng97]. The Shapemaker II process [Thomas96] also makes use of ruled surfaces to define the layer surfaces. Hope *et al.* [Hope97a] [Hope97b] create the appropriate contours using their own software, and obtain the cutting direction at discrete points

along the surface of a given layer by computing the cross product of the surface normal and the tangent vector at each.

The greatest disadvantage shared by these sloped layer methods is that they require a system with a minimum of four degrees of freedom (translations in the x-y plane and two rotational) to manufacture a given part. Adequate processes include wire EDM, hot-wire cutting, laser cutting, water-jet cutting, and CNC side milling, among others [de Jager97]. These systems are significantly more expensive and difficult to program than current 2½D rapid prototyping systems. Furthermore, although these methods significantly reduce stair-stepping, errors will persist for surfaces with double curvature [Hope97a].

Various other processes do not employ a machining stage to produce sloped layer surfaces, but simulate sloped layers instead. In the 3D Printing (3DP) process, layers are formed by spraying a binder onto a powder bed using inkjet technology. These binder droplets can be deflected during deposition to reduce the stair-stepping effect (further details have not been provided) [Sachs97].

Reeves *et al*. [Reeves97] simulate sloped layers using the Stereolithography Apparatus (SLA) by performing additional laser scanning sequences to cure meniscus regions between previously cured 2½D layers (Figures 2.14 and 2.15). The SLA fabricator employs an ultraviolet laser to selectively scan the surface of a vat of photopolymer resin. The scanned regions of the resin surface cure (or solidify) upon exposure to the laser beam to produce each build layer. Upon completion of each scanning sequence, a platform which supports the previously cured layers descends into the vat a distance equal to the subsequent build layer thickness (Figure 2.14). Time is allotted to allow the resin to settle above the top layer, and the scanning process is repeated. Reeves *et al*. employ additional scanning sequences to decrease the surface roughness of the part. Specifically, after completing each layer using the conventional process, they raise the build platform such that the most recently fabricated layer lies just above the resin surface. The resins' typically high surface tension causes a meniscus to form between the current layer and the one below it. This meniscus is then cured using additional scanning sequences (Figure 2.15) to reduce the stair-stepping error.

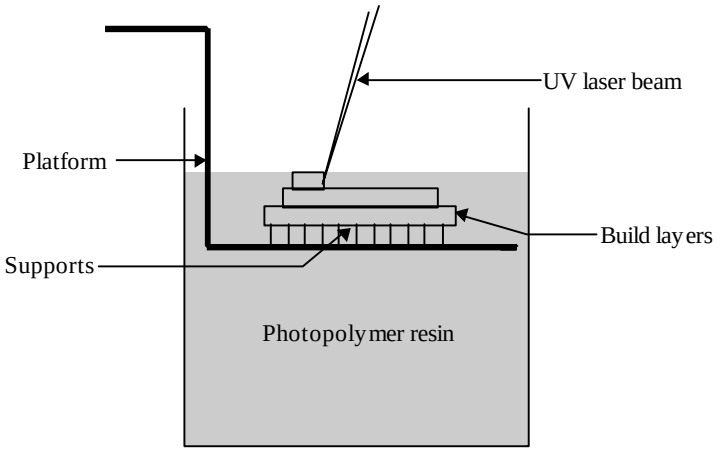

Figure 2.14: The Stereolithography Apparatus (SLA) creates each build layer by curing the surface of a vat of photopolymer resin with an ultraviolet laser.

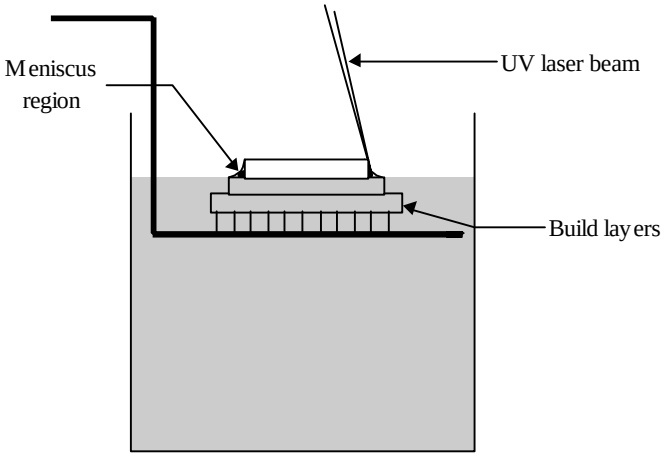

Figure 2.15: Curing the meniscus regions decreases the surface roughness.

2.7 OBSERVATIONS

With regard to manufacturing accurate parts in the minimum fabrication time using LM processes, the literature suggests the following:

(a) Although the .STL file format is the *de facto* industry standard, it suffers from a lack of topological information [Rock91a] [Rock92].

(b) Topology (connectivity) must be added to the facets, edges and vertices that comprise a solid to enable fast and efficient slicing processes [Rock91b].

(c) Adaptive slicing has been proven to reduce fabrication times while manufacturing parts with enhanced surface quality [Suh94] [Kulkarni95] [Kulkarni96] [Sabourin96a] [Sabourin96b] [Sabourin97].

(d) Employing stepwise uniform refinement, and specifically, evaluating the surface characteristics at every point along both the top and bottom slice levels of a given slab, makes it less likely to miss regions of extreme curvature during the slicing process [Sabourin96a] [Sabourin96b].

(e) Most conventional adaptive slicing procedures result in a needlessly inefficient build process. Specifically, the minimum build layer thickness computed along each slice level is used to fabricate all parts and individual part features existing at that height throughout the build envelope. This produces unnecessary build layers whenever any of these parts or features do not require this minimum layer thickness to meet the overall surface tolerance [Krause97].

CHAPTER 3

LOCAL ADAPTIVE SLICING

The new approach to local adaptive slicing minimizes the fabrication time required by adaptive layered manufacturing processes by identifying the individual parts and part features of a particular build and then determining an appropriate build layer thickness for each of them separately. The basic strategy employed by this local adaptive slicing technique incorporates three stages: (1) the generation of thick slabs, (2) the division of each thick slab into sub-slabs, and (3) the division of each sub-slab into a distinct number of thinner layers. The first and final stages are carried out similarly to the methods described in [Sabourin96a] [Sabourin96b] [Sabourin97]. The division of each thick slab into sub-slabs is accomplished by a contour matching algorithm that identifies contours from adjacent thick slices whose physical connectivity can be established using topology.

This chapter presents the methods upon which local adaptive slicing is based. Specifically, it briefly describes the thick slab generation process, details the contour matching algorithm, and revisits the stepwise uniform refinement method used to sub-divide each sub-slab. Finally, this chapter presents a comparison of the fabrication times resulting from the implementation of uniform slicing, conventional adaptive slicing, and local adaptive slicing techniques on several parts that were then fabricated on a FDM 1600 rapid prototyping system.

3.1 THICK SLAB GENERATION

This stage is comprised of several specific tasks. The first of these tasks involves loading a CAD model described in the .STL file format into memory. This task relies on the software libraries developed by Bøhn [Bøhn93b] to generate the needed topological information (using the topology reconstruction algorithm described in [Rock92]), and to ensure that the models are closed and properly oriented. The .STL file is then intersected with a series of horizontal planes,

or sliced, into uniformly thick slabs using the maximum thickness allowed by the fabricator. This slicing process employs the marching algorithm for slicing that is described in Section 2.3.

3.2 CONTOUR MATCHING

Sub-slabs are defined by two or more contours that are located on two adjacent slices and that are topologically connected in the vertical direction (Figure 3.1). Establishing this connectivity is essentially a many-to-many matching problem. This matching can be achieved by employing a multi-stage suite of tests applied in order of increasing computational cost (Figure 3.2), followed by a heuristic test to match the sub-slabs that connect horizontally within a given thick slab.

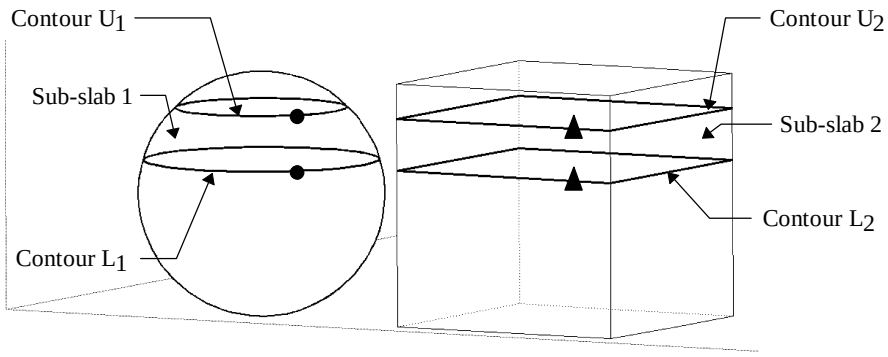

Figure 3.1: Lower contours L_1 and L_2 are paired with upper contours U_1 and U_2 to form sub-slabs 1 and 2 respectively. Sub-slab 1 can then be divided into *m* thinner layers, while sub-slab 2 is divided into *n* layers, with $m > n$.

The first two of this suite of tests seek to eliminate from consideration those contours that definitely cannot be matched; namely, those whose orientations are opposite and those that belong to different solids. If the contours have different orientations, then there cannot be a direct two-manifold connection between them contained between the two slice levels. Likewise, if the contours belong to different solids within the same build volume, then there cannot be a rigid connection between them. Determining the orientation of a closed, directed contour is well understood [O'Rourke94] and each contour can be tagged with its orientation, clockwise (CW) or counterclockwise (CCW), as it is generated. Thus, once the contours are tagged, it is trivial

and fast to check if they have the same orientation. The test for different solids is trivial and fast if shell membership is recorded with each facet during topology generation [Bøhn93a] [Bøhn93b]; simply compare the names of the shells that are pointed to by any of the facets associated with the contours in question.

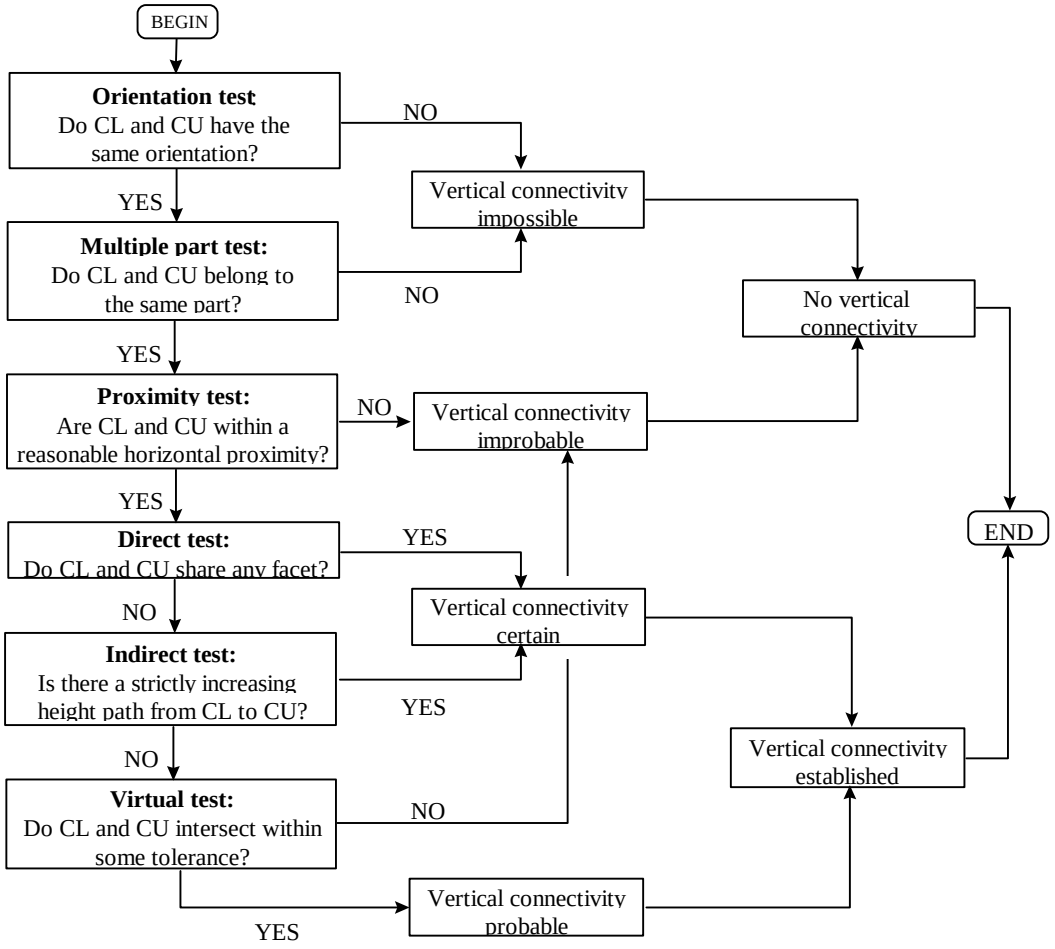

Figure 3.2: Checking for vertical connectivity between two contours located on adjacent slices.

The third test (or proximity test) is used to determine whether a vertical connection between the contours in question is probable. This test implies that it is unlikely for the contours to be vertically connected if they are separated by a horizontal distance (within the build volume) that is greater than a user-specified tolerance. A typical value for this tolerance is 1.0 inch (25.4 mm) when used with a slab thickness of 0.030 inches (0.76 mm).

The next two tests seek to establish definite topological contour connections in the vertical direction. In the direct test, each contour on the lower slice is searched for any facet that is also a member of a contour on the above adjacent slice. If such a facet exists, then the two contours in question both belong to the same sub-slab. For instance, in Figure 3.3, the contours C_L and C_U both belong to the same sub-slab. The direct test is fairly fast and will identify the majority of connections that exist since the probability of sharing at least one facet across the 0.030-inch (0.76 mm) slabs is high. In the minority of cases where the direct test fails to identify an existing connection, a computationally more expensive indirect test is applied. In particular, a steepest gradient climb upwards from each of the facets on the lower contours is performed in an attempt to reach the upper contours (Figure 3.4); if a connecting, strictly increasing ascent exists anywhere along the two contours, then they belong to the same sub-slab.

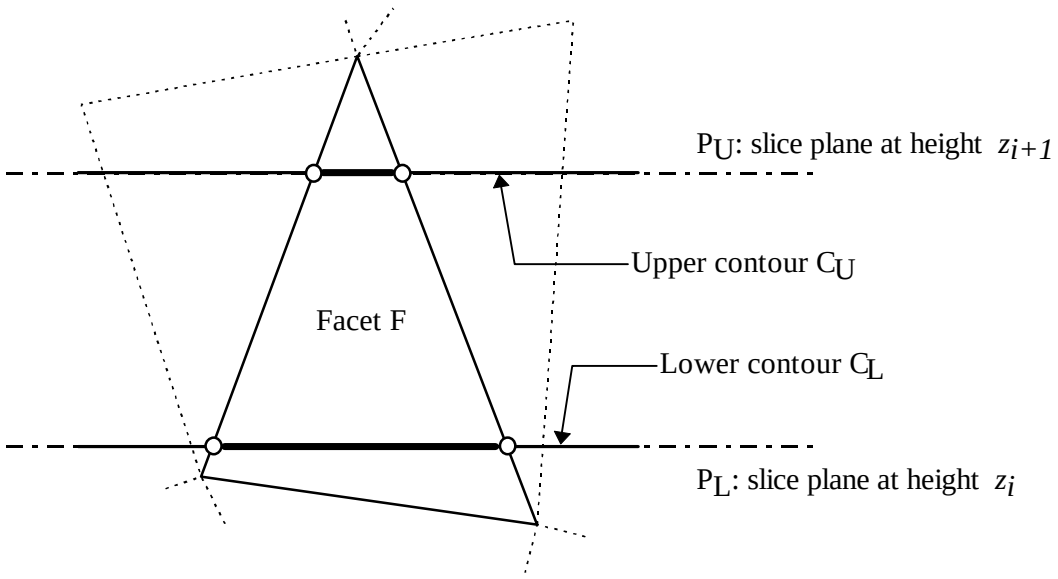

Figure 3.3: A shared facet F establishes connectivity between the two contours C_L and C_U located on the adjacent slices P_L and P_U, respectively.

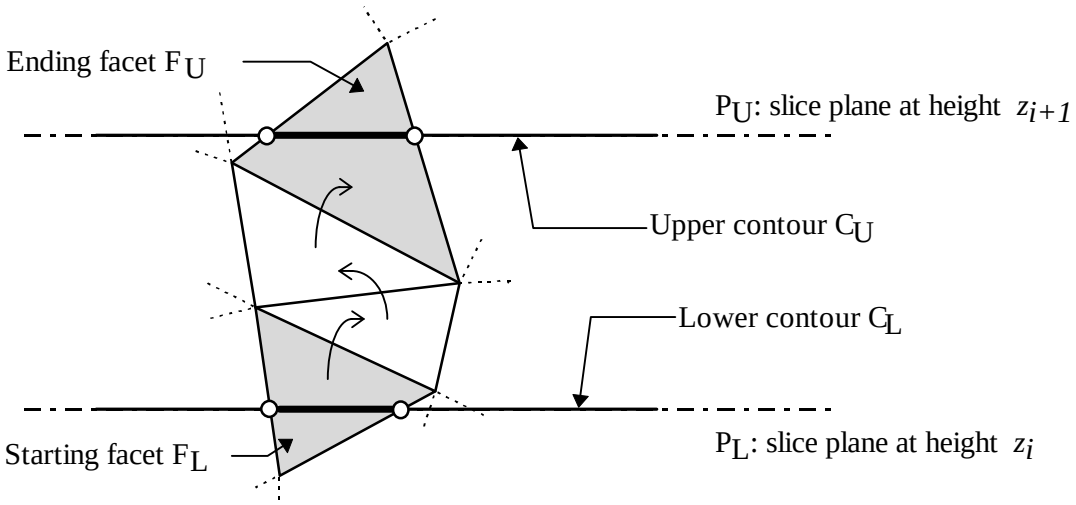

Figure 3.4: Adjacent facets can establish connectivity between the two contours C_L and C_U located on the adjacent slices P_L and P_U, respectively.

The final test seeks to resolve an uncertain, rare situation; namely when two contours are vertically connected without there being a single strictly increasing ascent between them (Figure 3.5). This situation is rare because the vertical difference between the slices is only 0.030 inches (0.76 mm), which is significantly smaller than most facets found in an .STL file. It is therefore improbable for .STL facets to describe a complex geometry within this space. Resolving this situation with certainty is computationally expensive. A conservative, but far less expensive solution is to consider that two contours belong to the same sub-slab if their projections onto a common horizontal plane intersect within some tolerance. In essence, a virtual connection is made between the two contours. This test is therefore referred to as the virtual test. This test will identify several special cases of vertical connectivity, and it may identify connectivities where none exist. When the latter happens, the fabrication will not fail, but will only cause the sub-slab to be fabricated with possibly thinner build layers than what is necessary to meet the specified surface tolerance.

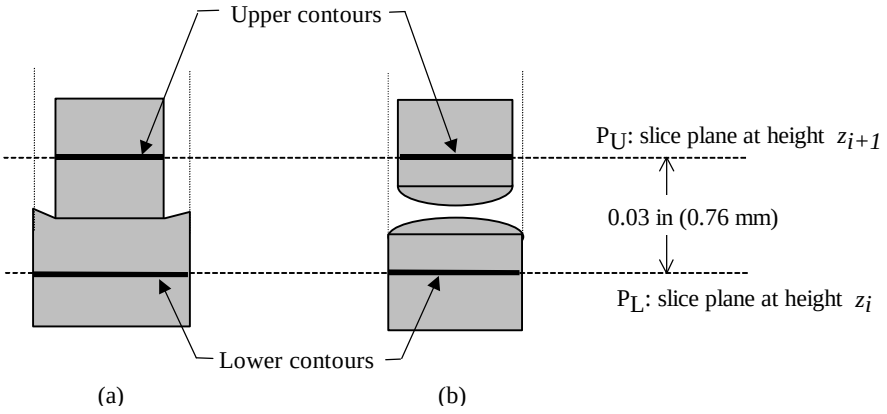

Figure 3.5: Instances when a virtual connection would be established. (a) Connection is correctly made; (b) rare occurrence where two features establish a false connection.

Once this suite of tests has been applied to each contour on a lower slice level with every contour on the adjacent slice level above it, the contours are organized into sub-slabs, each of which represent a many-to-many contour matching. This matching automatically accounts for branching and merging geometries, an example of which is shown in Figure 3.6. In this situation, all three contours (A, B and C) will comprise the given sub-slab and contribute to the calculation of an appropriate build layer thickness within that sub-slab. These contour matchings are all based on identifying two-manifold connectivity along the part surfaces.

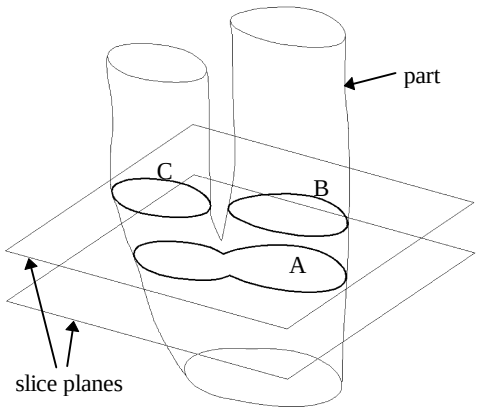

Figure 3.6: *Branching* occurs when a single contour at one thick slice plane is matched with multiple contours from the next highest slice plane.

In addition to establishing all vertical connections during the formation of sub-slabs, it is necessary to merge the sub-slabs within each thick slab based on their horizontal connectivity through solid material. In other words, each interior sub-slab must be matched with the appropriate exterior sub-slab on the same thick slab. To illustrate why these intra-slab connections are needed, consider the fabrication of an open, hollow, vertical cylinder. At each slice level there will be two contours, one for the outside surface and one for the inside surface. The contour matching algorithm presented thus far will connect the outer and inner contours into two separate sub-slabs, each of which would be refined separately. This, however, is incompatible with most layered manufacturing systems since they require that any area subject to material deposition fabrication (such as the material bound by these contours) be of constant thickness. Since the inner and outer sub-slabs formed by these contours are originally unconnected, there is no guarantee that their respective subsequent layer thicknesses will be identical. Fortunately, this can be remedied by merging the outer and inner sub-slabs based on the orientation of the contours on their lower slice levels. In the case of the cylinder, both sub-slabs would then be divided into the same number of uniform thickness build layers. Hence, the general solution is to match clockwise (CW) oriented inner contours with counterclockwise (CCW) oriented outer contours on the same slice level. This will effectively merge their respective sub-slabs (if different). Figure 3.7 illustrates this concept. The contours A, D, and F are each outer contours (CCW), while the contours B, C, and E are inner contours (CW). They will therefore be matched to form at most three sub-slabs containing {A,B,C}, {D,E}, and {F}, respectively.

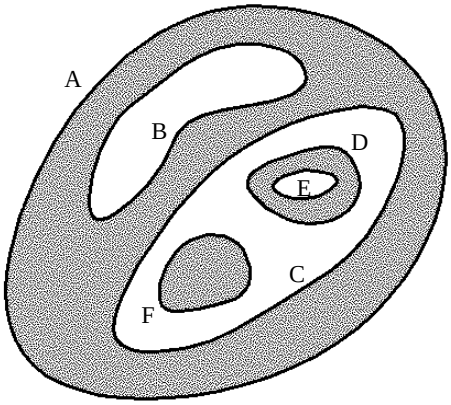

Figure 3.7: Interior and exterior contours in the same slice plane must be appropriately matched to ensure that the material between them is deposited with a single layer thickness. Each interior contour is matched with the smallest exterior contour that encloses it.

3.3 SUB-SLAB DIVISION

Once all sub-slabs have been defined, each sub-slab is subdivided independently into an integer number of uniform thickness build layers using the stepwise uniform refinement technique presented in [Sabourin96a] [Sabourin96b]. This number of thinner layers, $a_{\text{sub-slab}}$, is computed using the z-component of the unit surface normals at each point along the contours that make up the sub-slab:

$$a_{sub-slab} = \text{int}\left(\frac{L_{\max}}{C_{\max}}\max\{n_z\}\right) \quad a_{sub-slab} \in [1, a_{\max}] \quad a_{\max} = \text{int}\left(\frac{L_{\max}}{L_{\min}}\right) \tag{3.1}$$

where $L_{\min}$ and $L_{\max}$ are the minimum and maximum build layer thicknesses available, respectively; $C_{\max}$ is the maximum permissible surface error; and $\{n_z\}$ is the set of unit normal z-components for all the points along all the contours in the sub-slab. The build layer thickness used to fabricate this sub-slab therefore becomes:

$$l_{sub-slab} = \frac{L_{max}}{a_{sub-slab}} \tag{3.2}$$

With its build layer thickness determined, the sub-slab is efficiently sliced using the marching algorithm described in Section 2.3. Furthermore, the existence of sub-slabs eliminates the need for an extensive starting point search since suitable starting points are located along the sub-slab contours and, subsequently, along the vertical ascent up towards the top of the sub-slab. This will

suffice for those sub-slabs that were formed by either the direct or indirect test. However, for those that were formed by the virtual test, it is necessary to migrate the slicing both upward from the lower contours and downward from the upper contours since these might not actually be vertically connected. Likewise, feature tops and bottoms (Figure 3.8) only have contours on one side of the sub-slab. These will therefore have their build layer thicknesses extrapolated from the points along their contours on the one slice level only, and will only migrate the slicing away from that slice level.

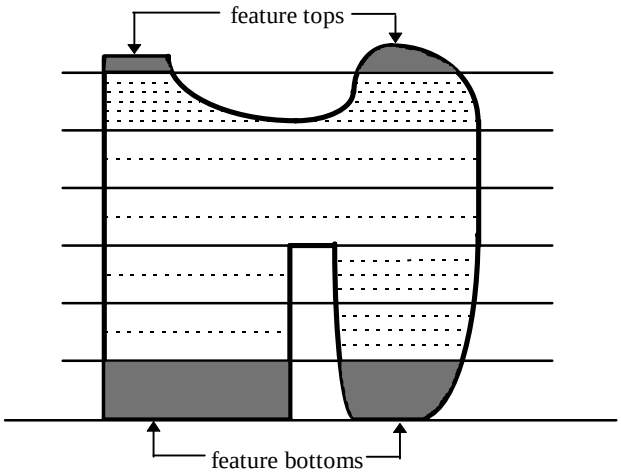

Figure 3.8: Feature tops and bottoms are identified as contours that do not connect to any contour in the slice plane above and below them, respectively.

3.4 RESULTS

The new approach to local adaptive slicing was implemented for the Stratasys, Inc. FDM 1600 rapid prototyping system. Software was written in C++ and compiled on an IBM RISC/6000 workstation using the xlC compiler under AIX 4.2. The program will slice any CAD model represented in the .STL file format. It currently generates the resulting slice contours in the .SSL file format for use with QuickSlice 5.0, the software provided by Stratasys, Inc. for generating NC code for their FDM systems.

The thickness used to generate the thick slabs was L_{max} = 0.030 inches (0.76 mm), corresponding to the maximum thickness permitted by the FDM 1600 rapid prototyping system.

The minimum layer thickness L_{min} was set to 0.005 inches (0.13 mm) which corresponds to an upper limit of 6 on $a_{sub-slab}$. In addition, the maximum cusp height C_{max} was set to

$$\frac{0.005''}{2}\sqrt{2} = 0.00354 \text{ inches } (0.09 \text{ mm}) \tag{3.5}$$

which corresponds to the cusp height generated by a 0.005 inch (0.13 mm) thick build layer modeling a 45° sloped surface (Figure 3.9).

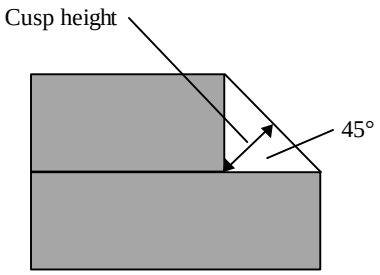

Figure 3.9: The maximum cusp height for a 45° sloped surface.

The software was configured for use with P400 ABS material with a 0.012 inch (0.30 mm) nozzle. Discrete layer thicknesses of 0.0050, 0.0075 and 0.0150 inches (0.13, 0.19 and 0.38 mm, respectively) were pre-defined for the thin layers into which the sub-slabs (0.03 inch or 0.76 mm) were sub-divided. Hence, each sub-slab was divided into either 6, 4 or 2 thinner layers having uniform thickness. In addition, the FDM 1600 system was calibrated according to the procedure outlined in the next Chapter. This was necessary to maximize the quality of parts fabricated using multiple build layer thicknesses simultaneously.

The new approach to local adaptive slicing realizes the most time savings when fabricating several complex and simple parts simultaneously. To illustrate this point, three configurations were fabricated using conventional adaptive slicing methods and, then again, using the new approach. The resulting sliced geometries for each of these builds are shown in Figures 3.10 and 3.11, respectively.

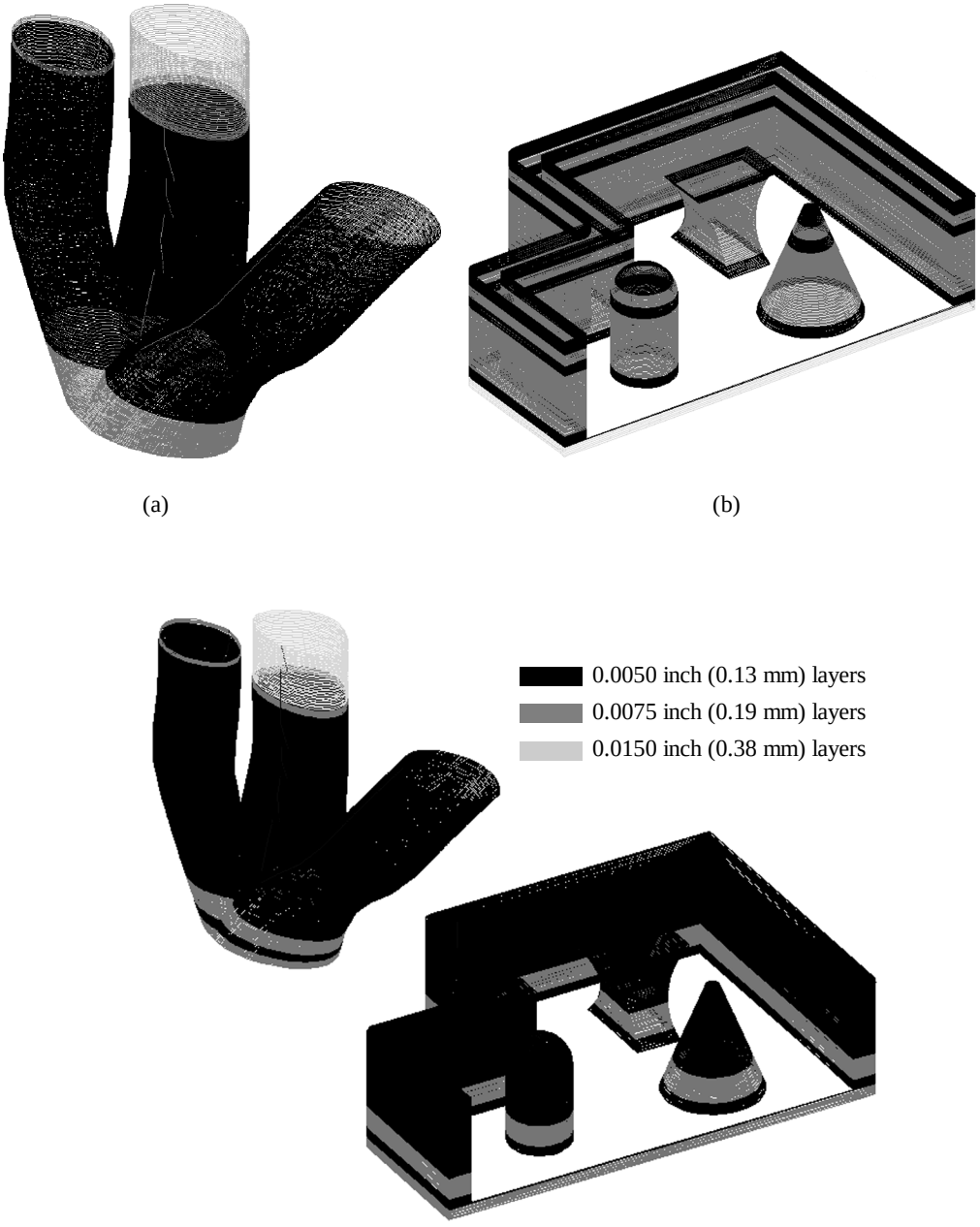

Figure 3.10: Sample builds using CAD models that were adaptively sliced using conventional methods. (a) Build 1 consists of part A; (b) build 2 consists of part B; and (c) build 3 consists of both parts A and B.

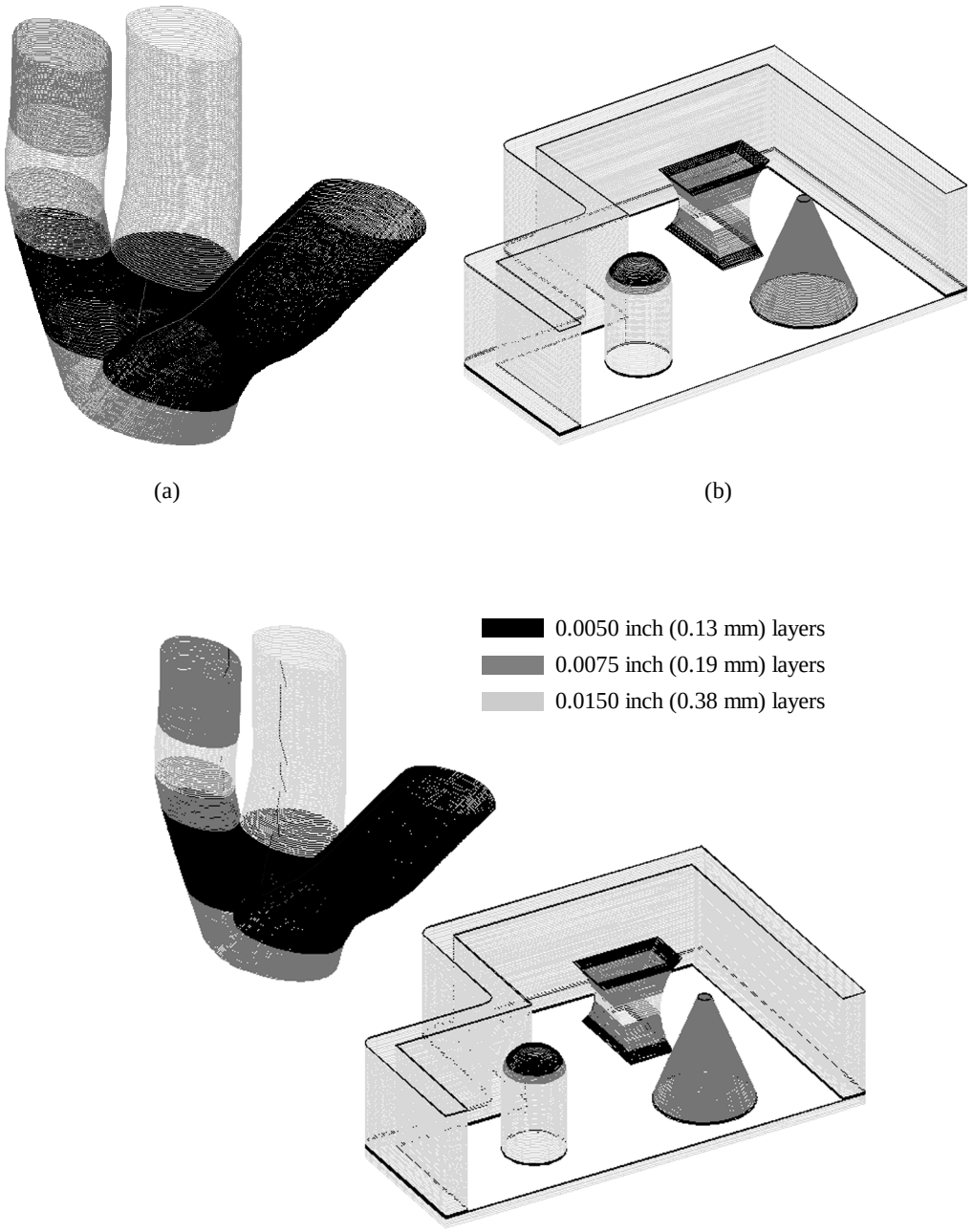

Figure 3.11: Sample builds using CAD models that were adaptively sliced using the new approach to local adaptive slicing. (a) Build 1 consists of part A; (b) build 2 consists of part B; and (c) build 3 consists of both parts A and B.

The first build consisted of a single part, part A, containing a base which branches into three individual features each having varying degrees of surface curvature. The second build also consisted of a single part, part B, comprised of predominantly vertical surfaces and several smaller, distinctly shaped features. Finally, the third build was the combination of both parts A and B. Each build was fabricated with the three discrete layer thicknesses mentioned above. These layer thicknesses are illustrated in Figures 3.10 and 3.11 using different shaded regions. The darkest, middle, and lightest regions of the figures denote the 0.0050 inch (0.13 mm), the 0.0075 inch (0.19 mm), and the 0.0150 inch (0.38 mm) thick layers, respectively.

Table 3.1 provides the fabrication times for each of the three builds using uniform slicing, conventional adaptive slicing, and the new local adaptive slicing routines. When using uniform slicing, the parts were built with 0.0050 inch (0.13 mm) layers in order to achieve the same level of part quality that the other two methods yield.

Table 3.1 Fabrication times of sample builds processed with various slicing methods.

Method	**Laver thicknesses** (in/mm)	**Fabrication times**					
		Build 1 (PART A)		**Build 2 (PART B)**		**Build 3 (PARTS A & B)**	
		(hours)	(relative)	(hours)	(relative)	(hours)	(relative)
Uniform Slicing	0.0050 / 0.13	11.1	100	13.3	100	24.1	100
Conventional Adaptive Slicing	0.0050 / 0.13 0.0075 / 0.19 0.0150 / 0.38	9.8	88	9.0	68	21.1	88
Local Adaptive Slicing	0.0050 / 0.13 0.0075 / 0.19 0.0150 / 0.38	8.1	73	5.6	42	13.2	55

For all experiments, both adaptive slicing techniques led to reduced fabrication times over uniform slicing. Furthermore, it was observed that the new local approach reduced the fabrication time for build 1 by an additional 15 percentage points as compared to the conventional method. Similarly, an additional savings of 26 percentage points was realized for build 2. However, the fabrication times for build 3 shows the real advantage of the new local approach over conventional adaptive slicing methods: An additional savings of 33 percentage points was realized when building parts A and B together. Figures 3.10 and 3.11 illustrate why this happens. Figure

3.10c, in particular, shows what happens when fabricating multiple parts using conventional adaptive slicing routines; the complex surfaces of part A cause nearly all of part B to be sliced with thinner layers than what Figure 3.11b indicates is necessary. On the other hand, the new local approach slices each part and feature of build 3 independently of the others, so each of the parts is sliced in exactly the same manner as when it was processed alone (Figure 3.11).

CHAPTER 4

CALIBRATION OF FUSED DEPOSITION RAPID PROTOTYPING SYSTEMS FOR FABRICATION WITH ADAPTIVE BUILD LAYER THICKNESSES

Commercial layered manufacturing (LM) systems have not been designed to accommodate either adaptive slicing or fabrication with adaptive build layer thicknesses. Most LM systems only support fabrication with uniform build layer thicknesses throughout a given build. Among these systems is the fused deposition modeler (FDM) rapid prototyping system developed by Stratasys, Inc., (Eden Prairie, Minnesota). For this system in particular, the standard calibrations of build parameters for different build layer thicknesses (provided by Stratasys) are out of alignment relative to one another.

This chapter considers calibration issues for existing FDM rapid prototyping systems. Both software and hardware issues are discussed. Specifically, this chapter briefly addresses the process required to implement adaptive slicing methods using this system. It then provides background information pertaining to FDM hardware, which includes an overview of initial attempts to fabricate with adaptive build layer thicknesses, and discusses the resulting poor part quality that prompted this study. This chapter then outlines experiments used to calibrate a FDM 1600 for fabrication of parts using adaptive build layer thicknesses. Finally, it provides data obtained from these experiments, and recommends specific build parameter values, based on these data, that help ensure robust fabrication with this system.

4.1 FDM SOFTWARE

QuickSlice, the postprocessor provided by Stratasys, Inc. for use with their FDM rapid prototyping systems, only supports uniform slicing routines; that is, it is only capable of slicing a CAD model with a single build layer thickness throughout. To take advantage of adaptive slicing techniques with this system, the user must implement independent adaptive slicing routines to generate the slices from a .STL file, and then output the results in the Stratasys slice file format (.SSL). Files in this format can then be imported by QuickSlice, which uses the slice data solely to generate the toolpaths necessary to drive the FDM hardware.

4.2 FDM 1600 HARDWARE

Layered manufacturing systems fabricate three-dimensional parts by adding layer upon layer of build material, beginning with the bottom of the part. The FDM rapid prototyping systems, in particular, achieve this by extruding molten wax or thermoplastic material through a small nozzle to form a thin bead or "road" that is deposited in a pre-determined pattern to complete each build layer, bonding the extrudate to adjacent and previously deposited roads. The motion of the extrusion system operates under three-dimensional computer numerical control (CNC). The extrusion system consists of a small ram extruder in which the spooled filament feedstock pushes molten material through the liquefier with low shear. The feedstock is driven into the extruder by counter rotating rollers as needed under CNC, where it is heated to a manually set temperature, T_L. The extrudate is deposited within a build chamber holding a manually set temperature, T_C. In the case of the FDM 1600 rapid prototyping system, T_L and T_C can be up to 300°C and 70°C, respectively.

The cross section of a FDM road has the shape of a flattened ellipsoid that can be approximated as a rectangle. Its height is given by the layer thickness, i.e., the height of the nozzle above previously deposited material. With this height being constant, the road width is controlled by the volumetric flow rate of the material through the liquefier and the speed of the liquefier (head) XY motion [Argawala96]. This flow rate is primarily dependent upon the ram speed, the material viscosity, and the nozzle tip dimensions [Comb94]; which can be manipulated

by varying the roller speed under CNC, by manually varying T_L, or by manually changing to a different nozzle size, respectively. Hence, for a constant material, nozzle, T_L and T_C combination, the road width can be determined by CNC of (1) the feed roller speed, (2) the build layer thickness, and (3) the head travel speed. This control can be pre-computed using QuickSlice [Stratasys97]. To manage these three parameters, QuickSlice uses look-up tables that are each based on a constant material, nozzle, T_L and T_C combination. For instance, given a liquefier head speed and build layer thickness, QuickSlice will use the lookup table calibrated for a specific material, nozzle, T_L and T_C combination, to determine the roller speed (flow rate) that most closely matches the user-requested road width. This function is shown in Figure 4.1 for the P400 ABS material (Stratasys, Inc.) on a FDM 1600 with a T_L of 270°C, a T_C of 70°C, a 0.012" (0.30 mm) nozzle, a head speed of 0.800 in/sec (20.3 mm/s), and build layer thicknesses of 0.0050", 0.0075", 0.0100", and 0.0150" (0.13 mm, 0.19 mm, 0.25 mm, and 0.38 mm), respectively.

Stratasys recommends using distinct nozzle diameters, liquefier temperatures T_L, and chamber temperatures T_C for various build layer thicknesses [Stratasys97]. However, these recommendations cannot be adhered to when building with multiple build layer thicknesses simultaneously, since these parameters cannot be varied under computer control during a given build. As a result, initial attempts to fabricate adaptively sliced parts while using the default parameters provided in Figure 4.1 produced (1) delamination, which occurs when consecutive build layers fail to bond to one another; (2) curling, which can be attributed to residual stresses in deposited material; (3) surface discontinuities that were particularly apparent when transitioning between adjacent build layers with dissimilar thicknesses; and (4) surface inaccuracies due to numerical round off.

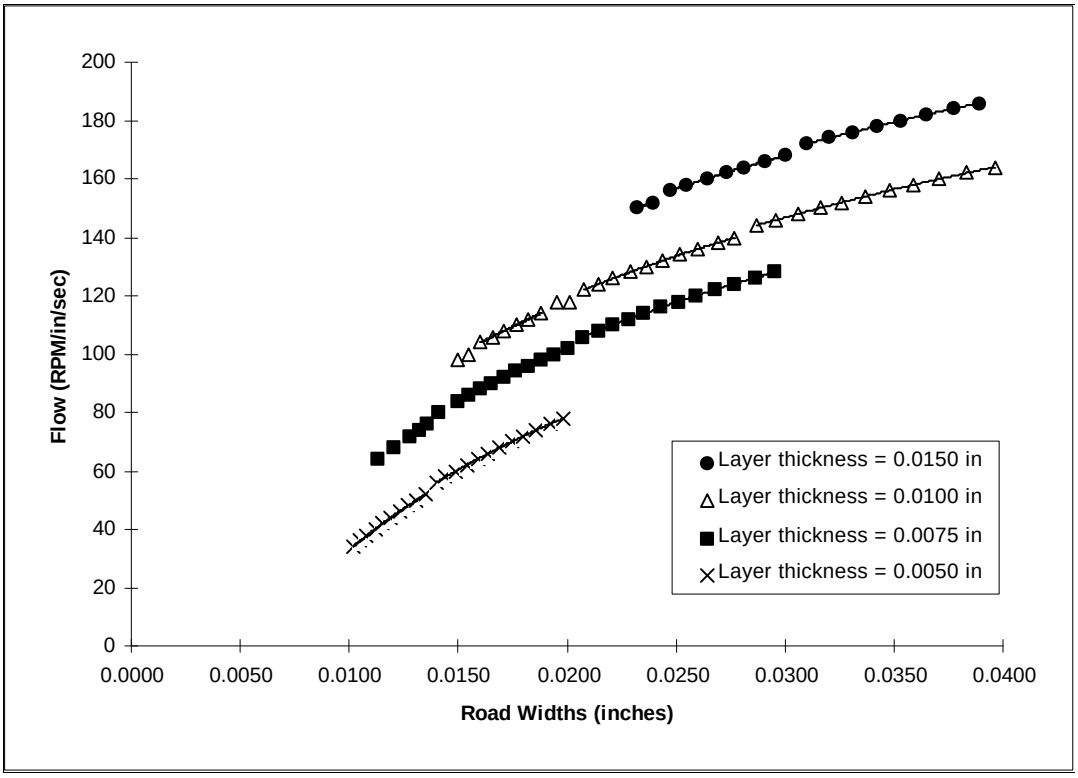

Figure 4.1: The flow rates and corresponding road width values predicted by QuickSlice for the extrusion of P400 ABS material through a 0.012 inch nozzle at liquefier and envelope temperatures of 270 and 70 (°C), respectively, with a constant liquefier head speed of 0.8 in/sec. The data can be represented by piecewise logarithmic functions.

Several factors contributed to the overall poor quality of these initial parts. Figure 4.1 explains one reason why the surface discontinuities occur. Ideally, the functions relating the flow rate to the road width should be continuous, both along a curve (reflecting a change in road width for a given build layer thickness) and from one curve to another (reflecting the transition from one build layer thickness to another). This, however, is clearly not the case for the QuickSlice lookup tables (Figure 4.1) which effectively describe a set of piecewise logarithmic curves (solid curves). One would expect, as is the case, that road widths calculated from these discontinuous build layer curves will be slightly off target. Furthermore, experiments (described in the next Section) indicate that, for a given nozzle diameter, the liquefier and chamber temperature settings have a significant effect on the road width values obtained using particular flow rates and build layer thicknesses. Indeed, these effects must be accounted for if the build layer thicknesses are to be

properly calibrated with respect to one another. Finally, the issue of conflicting build parameters for different build layer thicknesses must be resolved in order to fabricate high quality parts when using these thicknesses simultaneously.

Past work in FDM calibration has not addressed these particular issues, probably because researchers have not been concerned with fabricating with multiple build layer thicknesses simultaneously. Comb *et al*. [Comb94] discuss various control and material selection parameters that affect the overall FDM process; Agarwala *et al*. [Argawala96] address the internal and surface defects that lead to poor structural quality of parts produced by fused deposition systems; while Yardimici *et al*. [Yardimici97] present a thermal analysis of the extrusion process of FDM systems and the effect of liquefier and nozzle designs on these systems.

4.3 CALIBRATION EXPERIMENTS

Two sets of experiments were conducted using a FDM 1600 rapid prototyping system loaded with P400 ABS material. The first was designed to gather accurate data pertaining to the relationship between various feed roller speeds (flow rates) and their resulting road widths for various build layer thicknesses. The second was designed to assess the effect of T_L and T_C combinations, build style, and flow rate values on the overall part quality.

4.3.1 Determining Road Width vs. Flow Rate

Road width measurements were obtained by building several series of vertical walls. Each wall was 2.0" (50 mm) long, 0.25" (6.4 mm) tall, had the width of a single bead, and was assigned a flow rate value being an even number between 2 and 254 (RPM/inch/sec) [Stratasys97]. Each series contained up to 21 parallel walls that were given sequentially increasing flow rates, and that were located about 0.4" (10 mm) apart on a single support material base. This base was placed in the center of the build chamber, and its walls were oriented in the direction of the heated airflow in the build chamber, to provide near uniform material cooling.

12 series of walls were fabricated using a nozzle tip diameter of 0.012" (0.30 mm); T_L / T_C settings of 270°C / 70°C, 290°C / 70°C, and 290°C / 50°C; and build layer thicknesses of

0.0050", 0.0075", 0.0100", and 0.0150" (0.13 mm, 0.19 mm, 0.25 mm, and 0.38 mm). The flow rates comprised all even numbers between 50 and 90, 70 and 110, 112 and 140, and 130 and 170, for the 0.0050", 0.0075" 0.0100", and 0.0150" (0.13 mm, 0.19 mm, 0.25 mm, and 0.38 mm) build layer thickness, respectively. The head speed was kept constant at 0.800 in/sec (20.3 mm/sec). The external ambient conditions were measured with a thermometer and hydrometer on top of the FDM 1600. The temperature measured between 78°F and 80°F (25°C and 27°C), and the relative humidity measured between 25% and 32%.

Five measurements were taken from each wall using a caliper with a 0.0005" (0.01 mm) resolution. All measurements were obtained from the central regions of the walls to ensure that only steady-state deposition was being measured. All measurements are shown in Figure 4.2, and each data series representing a different temperature setting was given a trendline using Microsoft Excel 7.0.

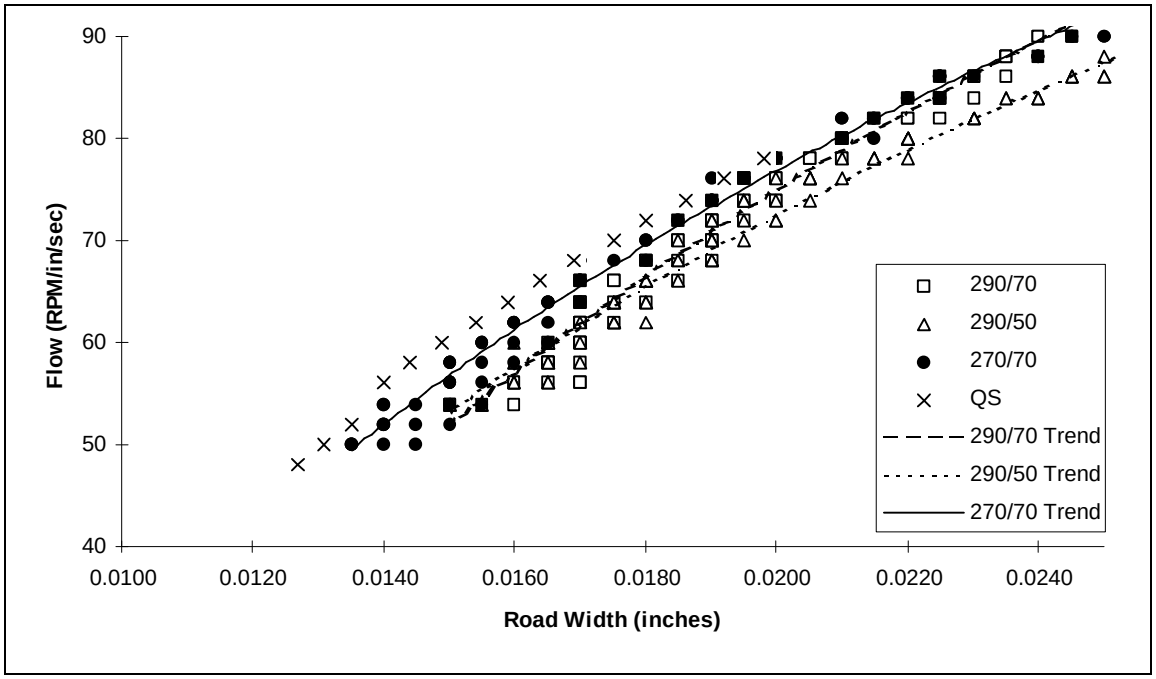

(a) layer thickness = 0.0050 inches

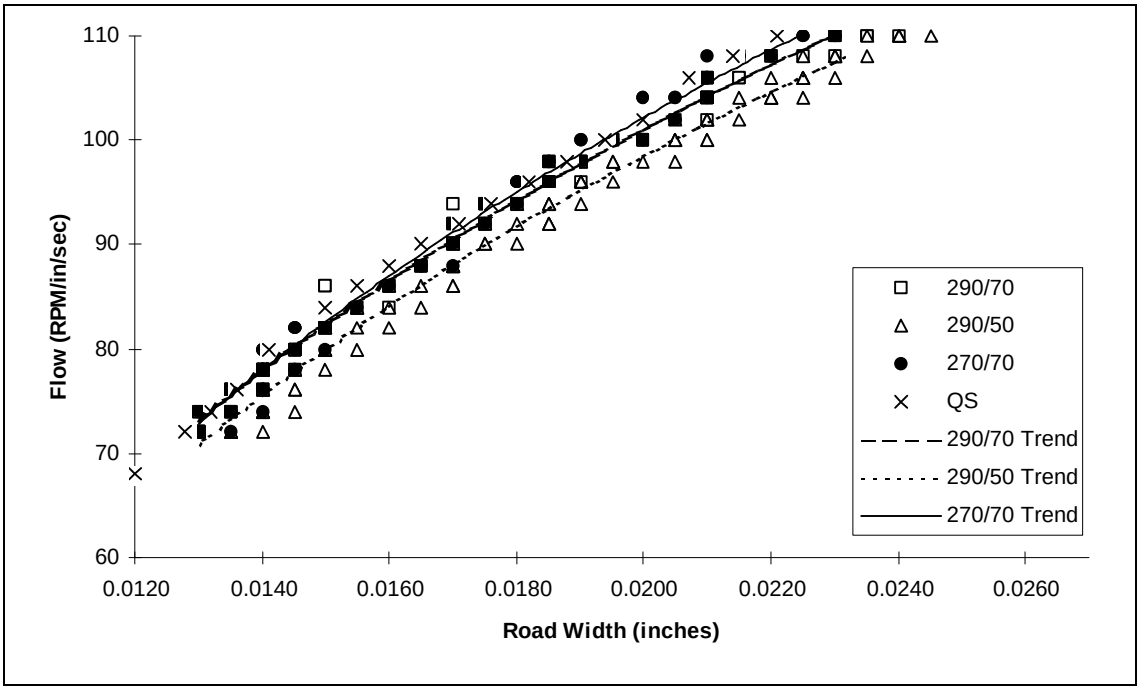

(b) layer thickness = 0.0075 inches

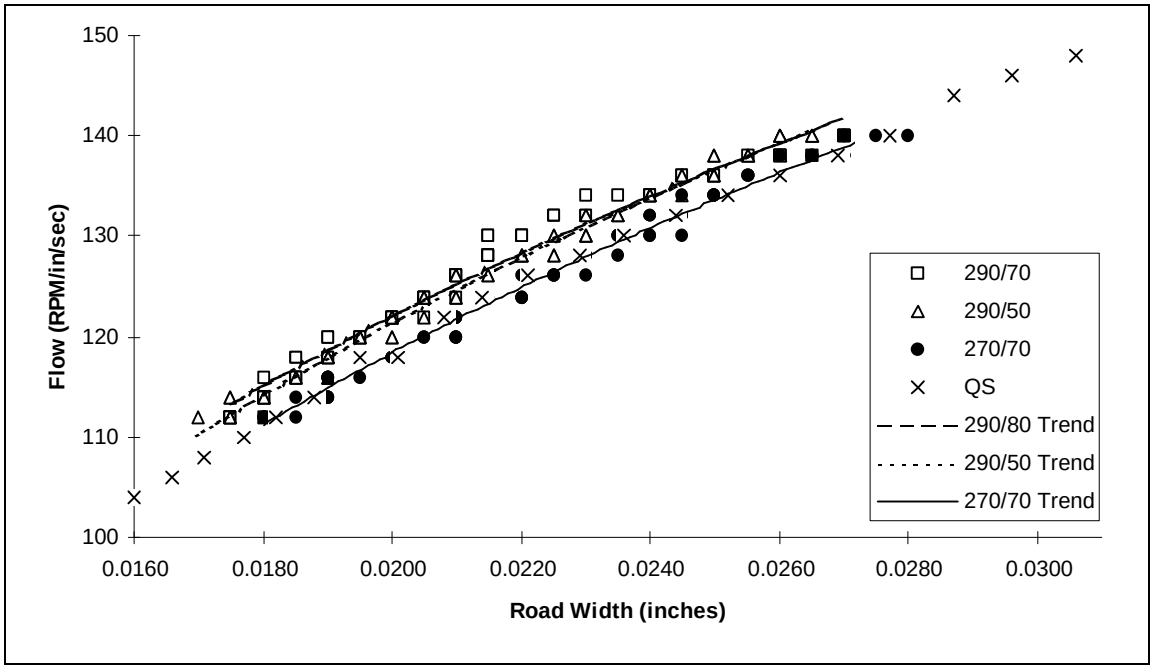

(c) layer thickness = 0.0100 inches

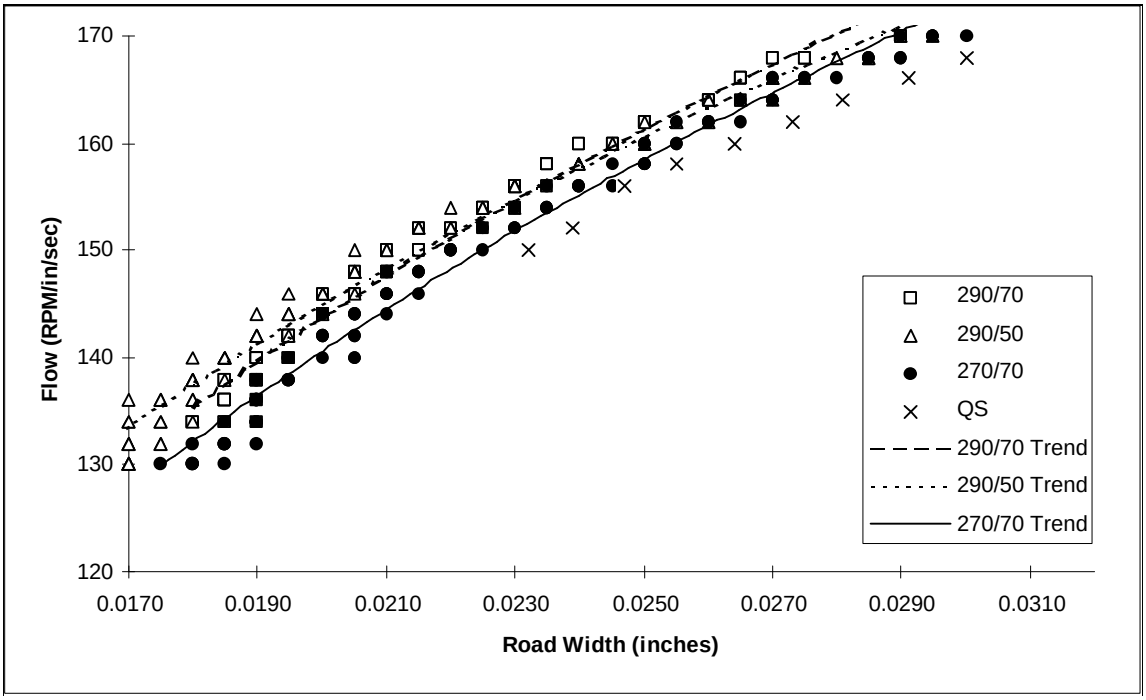

(d) layer thickness = 0.0150 inches

Figure 4.2: Experimentally collected road width values for specified flow rates at various liquefier and envelope temperature settings (°C) using P400 ABS material, a 0.012 inch nozzle, and a constant liquefier head speed of 0.8 in/sec.

4.3.2 Assessing Effects of Build Parameters on Overall Part Quality

A solid 1.0" × 1.0" × 0.72" (25 mm × 25 mm × 18 mm) test block consisting of 36, 24, 18, and 12 0.0050", 0.0075", 0.0100", and 0.0150" (0.13 mm, 0.19 mm, 0.25 mm, and 0.38 mm) build layers, respectively, was fabricated repeatedly to assess the specific build parameters T_L, T_C, build style, and flow rate, on the overall part quality. Five samples of this block were built using a 0.012" (0.30 mm) nozzle, 0.800 in/sec (20.3 mm/sec) head speed, and the respective parameters listed in Table 4.1. The T_L / T_C were set at 270°C / 70°C and 290°C / 50°C since Stratasys, Inc. recommends these values for fabricating with 0.0100" (0.25 mm) and 0.0070" (0.18 mm) build layer thicknesses, respectively [Stratasys97]. The build styles tested were contour, where the roads were deposited first at the perimeter and then progressively in towards the center for each layer, and raster patterns. Each of the five parts was built in the same location and orientation in

the center of the build chamber to minimize the possible effects of non-uniform transverse cooling.

Table 4.1: Build parameter sets used for experimental builds.

Part	Build Style	Liquefier/Envelope Temp. Settings (°C)	Flow Rate/Road Width (in) Values 0.0050	0.0075	0.0100	0.015
A	contour (Out-In)	270/70	56/0.014	78/0.014	118/0.020	140/0.020
B	contour (Out-In)	270/70	76/0.020	102/0.020	118/0.020	140/0.020
C	Raster	270/70	76/0.020	102/0.020	118/0.020	140/0.020
D	Raster	290/50	56/0.014	78/0.014	118/0.020	140/0.020
E	Raster	290/50	76/0.020	102/0.020	118/0.020	140/0.020

4.4 RESULTS

4.4.1 Road Width Calibration

Figure 4.2 shows that discrepancies exist between the experimental road width data and the default data used by QuickSlice. The most significant discrepancies are due to changes in the T_L and T_C settings. However, for the 0.0050" (0.13 mm) and 0.0150" (0.38 mm) build layer thicknesses, the QuickSlice data are inconsistent with any temperature setting (Figures 4.2a and 4.2d); in the first case with the QuickSlice estimated road width being less than the measured road width, while in the latter case it being opposite. Furthermore, Figure 4.2c shows that the QuickSlice road width estimates perfectly match the experimental data for the 0.012" (0.30 mm) nozzle, 0.010" (0.25 mm) build layer thickness, 0.020" (0.51 mm) road width, and T_L / T_C of 270°C / 70°C combination; which is the standard build parameter combination recommended by Stratasys, Inc. [Stratasys97]. These results explain (1) why Stratasys, Inc. prefers that customers consistently use the standard parameter combination, and (2) why current QuickSlice flow rates and road widths perform poorly when used in adaptive slicing.

Figure 4.2 shows that a 20°C increase in liquefier temperature T_L from 270°C to 290°C reduces the measured road width by about 0.001" (0.025 mm) in the cases of 0.0100" (0.25 mm) and 0.0150" (0.38 mm) build layer thicknesses, while it has only an insignificant effect in the cases of 0.0050" (0.13 mm) and 0.0075" (0.19 mm) build layer thicknesses. It also shows that a 20°C decrease in build chamber temperature T_C from 70°C to 50°C increases the measured road width

by nearly 0.001" (0.025 mm) in the cases of 0.0050" (0.13 mm) and 0.0075" (0.19 mm) build layer thicknesses, while it has only an insignificant effect in the cases of 0.0100" (0.25 mm) and 0.0150" (0.38 mm) build layer thicknesses. Finally, Figure 4.2 shows that when combining these changes in T_L and T_C the measured road width increased by about 0.001" (0.025 mm) in the cases of 0.0050" (0.13 mm) and 0.0075" (0.19 mm) build layer thicknesses, and decreased by about the same amount in the cases of 0.0100" (0.25 mm) and 0.0150" (0.38 mm) build layer thicknesses.

Increasing T_L will, for thick roads, add heat to the extrudate, and thus increase the time during which the material experiences significant shrinkage. Thick roads will therefore shrink as T_L increases. Thin roads, on the other hand, will continue to cool down too fast to significantly increase shrinkage, and they will therefore not experience a change in measured road width.

Decreasing T_C will, for thin roads, prevent the extrudate from heating up existing material to above the softening point (105°C). The existing material will therefore not yield to the pressure exerted by the extrudate, which causes the extrudate to escape outwards to create a wider road. Thick roads, on the other hand, contain sufficient heat so the extrudate can continue to bring existing material to above the softening point. This causes the existing material to continue to yield to the extrudate pressure, and hence there is no change in measured road width.

4.4.2 Effects of Numerical Round Off

Imperfect surface transitions between adjacent build layers of dissimilar thicknesses can also be caused by numerical round off. The flow rates selected represent discrete road widths at given build layer thicknesses. These road widths can be carried through the road path calculations as high resolution floating point numbers, and up until this point, any numerical round off would be insignificant. However, these floating point values need, in the case of current FDM equipment, to be rounded off to the closest 0.001" (0.025 mm) XY coordinate to reflect the programming resolution of the FDM's XY controller. This round off can easily cause a 0.001" (0.025 mm) mismatch within any two build layers. This mismatch will in general be particularly noticeable between two adjacent build layers of dissimilar thicknesses since the round off error adds to errors

in the road width estimation function (however small they might be, they will most likely be present). Figure 4.3 illustrates this problem.

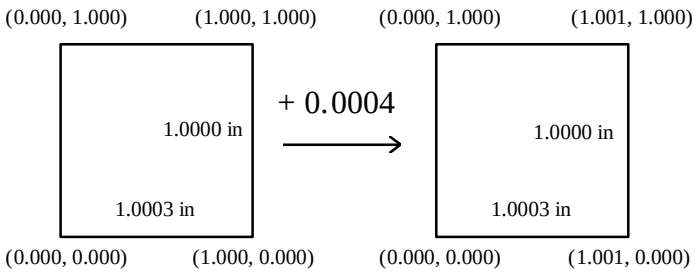

Figure 4.3: Numerical round off can change final fabricated dimensions, here shown for a 1.0003" ´ 1.0000" rectangle before and after a 0.0004" translation in the X direction.

Consider a rectangular cylinder measuring 1.0003" × 1.0000" (25.408 mm × 25.400 mm). Due to numerical round off, it will be manufactured as a perfect 1.000" × 1.000" (25.400 mm × 25.400 mm) square. Now move the original cylinder 0.0004" (0.010 mm) in the positive X direction. This would simulate the change in road path offset due to a slight change in road width, which invariably occurs as one transitions from one build layer thickness to another. The size of the virtual cylinder will thus remain the same; however, the new manufactured cylinder will now measure 1.001" × 1.000" (25.425 mm × 25.400 mm) and will no longer be perfectly square.

The build layer thickness transitional errors appeared to being limited to not much more than that which arises from numerical round off. This was in part determined by using a sheet of paper (0.0035", 0.09 mm) to gauge the relative magnitude of the build layer thickness transitional surface discontinuities.

4.4.3 Overall Part Quality

As described in the previous Section, a 1.0" x 1.0" x 0.72" test block was fabricated five times. Each test block consisted of 36 0.0050" (0.13 mm), 24 0.0075" (0.19 mm), 18 0.0100" 0.25 mm), and 12 0.015" (0.38 mm) layers, with the layer thicknesses increasing in the vertical (z) direction. Each build implemented a set of parameters given in Table 4.1. Profiles of the resulting parts, **a** through **e**, are shown in Figures 4.4a-e, respectively. By comparing these individual

parts, it can be concluded that the highest part quality is obtained using a raster build style with T_L = 290°C (Figures 4.4d,e). It was also found that part quality improved if the build chamber temperature T_C simultaneously was reduced to 50°C, which is in accordance with the recommendations provided by Stratasys, Inc. for fabricating with 0.007" (0.18 mm) build layers [Stratasys97]. In addition, a thicker road width seems better suited for the 0.0050" and 0.0075" (0.13 and 0.19 mm) layer thicknesses when using the 0.0120" (0.30 mm) tip. Hence, the flow rates for these layers must be adjusted because they are originally set by Stratasys to produce road widths of 0.014" (0.36 mm).

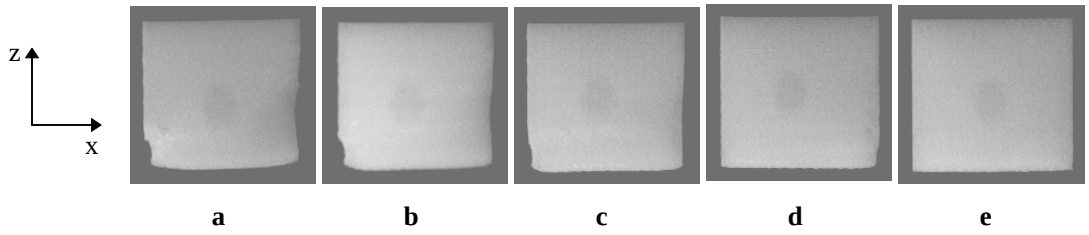

Figure 4.4: Parts fabricated from adaptively sliced geometry using P400 ABS plastic material and the parameter sets given in Table 4.1.

It should be noted that the 0.0050" and 0.0075" (0.13 and 0.19 mm) layers contributed most to the poor quality of each part, especially at the lower liquefier temperature (Figures 4.4a-c). This is likely the result of increased viscoelastic stresses in the deposited material of these thinner layers. Fortunately, the curling and delamination effects are virtually eliminated when increasing the liquefier temperature (Figures 4.4d,e).

Sperling [Sperling92] presents the viscosity of polymer material as

$$h = Ae^{\frac{E_a}{RT}} \tag{4.1}$$

where A is a material specific constant, E_a is the activation energy of the polymer, R is the universal gas constant, and T is the absolute temperature of the material. Furthermore, he expresses the relaxation time of polymers as

$$t = \frac{h}{E} \tag{4.2}$$

where E is Young's modulus. Finally, the viscoelastic behavior of the material can be modeled as

$$s = s_o e^{-\frac{t}{t}} \tag{4.3}$$

where s represents the mechanical stresses in the material, and t represents time.

From these equations, it can be observed that increasing the temperature of the extrudate decreases its viscosity, thereby reducing the relaxation time of the polymer, which subsequently reduces its mechanical stresses. Hence, the curling and delamination that was present in parts **a**, **b** and **c** is significantly reduced for parts **d** and **e**, which were built at the higher liquefier temperature. Thus, it is recommended that the liquefier temperature be increased when fabricating with multiple build layer thicknesses simultaneously in order to accommodate the higher viscoelastic stresses of the thinner layers used.

CHAPTER 5

CONCLUSIONS AND CONTRIBUTIONS

This thesis has presented a new method that significantly reduces the fabrication time associated with conventional adaptive slicing procedures. It has also presented a calibration procedure for the Fused Deposition Modeler rapid prototyping system that facilitates the fabrication of accurate, adaptively sliced parts by improving the dimensional accuracy of the transitions between different layer thicknesses, and by identifying build parameters that help ensure high part quality. Actual parts have been produced to demonstrate both aspects of this work. This research represents important steps toward the realization of a truly fast and accurate layered manufacturing process.

5.1 CONCLUDING REMARKS

The new approach to adaptive slicing, presented in this thesis, is limited to polyhedral CAD models such as those described in the .STL file format. The .STL format, however, is the *de facto* industry standard and is supported by all commercial layered manufacturing systems. Therefore, the new approach could be implemented in any of these LM processes, provided that the software is modified to output the slice data in the appropriate format. Currently, the software generates slice data for the FDM rapid prototyping system only.

The potential advantage that can be realized by this new method is critical to the layered manufacturing industry. In particular, users of FDM systems may benefit from enormous savings in fabrication time. The potential for savings is directly proportional to the number of individual parts and/or part features in a given build, and their respective differences in geometry. Hence, this new method is ideal for users in industry who typically optimize fabrication by building multiple parts simultaneously.

5.2 CONTRIBUTIONS

This thesis addresses the inefficiencies of current adaptive slicing procedures, as well as the issue of reducing these procedures to practice. Specifically, this thesis has made the following contributions:

Efficient adaptive layered manufacturing: The feasibility and advantage of adaptively slicing individual parts and part features independently of one another has been demonstrated. This new method overcomes the limitations of conventional adaptive slicing routines by accounting for differences in surface geometry in three dimensions. Rather than consider only the differences in surface geometry from one height to the next, the new procedure utilizes topology-based feature extraction to separate individual surfaces at each build height so that they may be treated independently. The result is the elimination of unnecessary layers and, hence, reduced fabrication times.

FDM calibration for adaptive build layer thicknesses: The ability to manufacture accurate, adaptively sliced parts using the FDM system has been demonstrated. In particular, a calibration procedure has been presented that reduces the inaccuracies that occur when transitioning between dissimilar build layer thicknesses. Prior to this work, commercial layered manufacturing systems have not supported multiple build layer thicknesses concurrently. Consequently, little concern has been given to the variations in calibration accuracy when transitioning from one layer thickness to another. This thesis has demonstrated that this variation in calibration should be of concern, and it has demonstrated how these problems can be overcome. Specifically, experiments have been conducted to determine the effects of critical FDM build parameters, including the flow rate, and the liquefier and chamber temperatures, on the quality of fabricated parts. These observations were then used to recommend parameter values that will consistently produce highly accurate parts.

5.3 RECOMMENDATIONS FOR FUTURE WORK

This thesis presents important contributions to the layered manufacturing industry; however, several aspects must be properly completed to ensure its acceptance. The following should be investigated:

Support generation: Fabrication of overhang structures requires that temporary support structures be built. At present, the new local adaptive slicing procedure does not have a companion support generation procedure that is capable of generating support structures for locally adaptive parts. Developing such a support generation procedure is non-trivial. Consider, for example, the merging of two features that require support structures, and whose surfaces call for different build layer thicknesses. Such an occurrence would cause support layers of different thicknesses to merge as well. At a minimum, a method that possesses the ability to adequately handle this and other situations when generating support structures must be developed before parts that require them can be manufactured.

Incorporation with existing methods: Several adaptive slicing methods have been introduced which enhance the speed and accuracy of layered manufacturing processes. Some of these make good candidates for integration with the approach developed in this thesis. Specifically, the incorporation of the high-precision exterior, high-speed interior layered manufacturing process developed by Sabourin *et al*. [Sabourin96a] [Sabourin97] would produce a truly efficient fabrication process.

REFERENCES

[Argawala96] Argawala, M. K., Jamalabad, V. R., Langrana, N. A., Safari, A., Whalen, P. J., and Danforth, S. C., "Structural Quality of Parts Processed by Fused Deposition," *Rapid Prototyping Journal*, vol. 2, no. 4, 1996, pp. 4-19.

[Beaman97] Beaman, J. J., Barlow, J. W., Bourell, D. L., Crawford, R. H., Marcus, H. L., and McAlea, K. P., *Solid Freeform Fabrication: A New Direction in Manufacturing*, Klewar Academic Publishers, Norwell, Massachusetts, USA, 1997.

[Bøhn89] Bøhn, J. H., "Computing the Unit Normal for NURBS Surfaces," M.S. Thesis, Rensselaer Polytechnic Institute, Troy, New York, USA, December, 1989.

[Bøhn93a] Bøhn, J. H., and Wozny, M. J., "A Topology-Based Approach for Shell-Closure," in: Wilson, P. R., *et al.*, eds., *Geometric Modeling for Product Realization*, IFIP Transactions B-8, Elsevier Science Publishers B. V. (North-Holland), Amsterdam, 1993, pp. 297-319.

[Bøhn93b] Bøhn, J. H., *Automatic CAD Model Repair*, Ph.D. thesis, Rensselaer Polytechnic Institute, Troy, New York, USA, August 1993.

[Brock91] *STH File Format*, Brock Rooney and Associates, Inc., Birmingham, Michigan, USA, 1991.

[Burns93] Burns, M., *Automated Fabrication; Improving Productivity in Manufacturing* , PTR Prentice Hall, Englewood Cliffs, New Jersey, USA, 1993.

[CLI98] Common Layer Interface (CLI), version 2.0, Available: http://www.cranfield.ac.uk/coa/rapid/cli/cli_v20.html [January 22, 1998].

[Comb94] Comb, J. W., Priedeman, W. R., and Turley, P. W., "FDM Technology Process Improvements," *Proceedings, Solid Freeform Fabrication Symposium* , Marcus, H. L., *et al.*, eds., University of Texas at Austin, Austin, Texas, USA, August 8-10, 1994, pp. 42-49.

[de Jager97] de Jager, P. J., Broek, J. J., and Vergeest, J. S. M., "Using Adaptive Ruled Layers for Rapid Prototyping: Principles and First Results," *Proceedings, Solid Freeform Fabrication Symposium*, Bourell, D. L., *et al*., eds., University of Texas at Austin, Austin, Texas, USA, August 11-13, 1997, pp. 585-592.

[Dolenc94] Dolenc, A. and Mäkelä, I., "Slicing Procedures for Layered Manufacturing Techniques," *Computer-Aided Design*, vol. 26, no. 2, February 1994, pp. 119-126.

[Fadel96] Fadel, G. M., and Kirschman, C., "Accuracy Issues in CAD to RP Translation," *Rapid Prototyping Journal*, vol. 2, no. 2, 1996, pp. 4-17.

[Guduri92] Guduri, S., Crawford, R. H., and Beaman, J. J., "A Method to Generate Exact Contour Files for Solid Freeform Fabrication," *Proceedings, Solid Freeform Fabrication Symposium*, Marcus, H. L., *et al*., eds., University of Texas at Austin, Austin, Texas, USA, August 3-5, 1992, pp. 95-101.

[Hope97a] Hope, R. L., Jacobs, P. A., and Roth, R. N., "Rapid Prototyping with Sloping Surfaces," *Rapid Prototyping Journal*, vol. 3, no. 1, 1997, pp. 12-19.

[Hope97b] Hope, R. L., Jacobs, P. A., and Roth, R. N., "Adaptive Slicing with Sloping Layer Surfaces," *Rapid Prototyping Journal*, vol. 3, no. 3, 1997, pp. 89-98.

[Jamieson95] Jamieson, R., and Hacker, H., "Direct Slicing of CAD Models for Rapid Prototyping," *Rapid Prototyping Journal*, vol. 1, no. 2, 1995, pp. 4-12.

[Keppel75] Keppel, E., "Approximating Complex Surfaces by Triangulation of Contour Lines," *IBM Journal of Research and Development* , vol. 19, no. 1, pp. 2-11.

[Kirschman92] Kirschman, C. F., and Jara-Almonte, C. C., "A Parallel Slicing Algorithm for Solid Freeform Fabrication Processes," *Proceedings, Solid Freeform Fabrication Symposium*, Marcus, H. L., *et al*., eds., University of Texas at Austin, Austin, Texas, USA, August 3-5, 1992, pp. 26-33.

[Klingbeil97] Klingbeil, N. W., Zinn, J. W., and Beuth, J. L., "Measurement of Residual Stress in Parts Created by Shape Deposition Manufacturing," *Proceedings, Solid*

Freeform Fabrication Symposium, Bourell, D. L., *et al*., eds., University of Texas at Austin, Austin, Texas, USA, August 11-13, 1997, pp. 125-132.

[Krause97] Krause, F. L., Ulbrich, A., Ciesla, M., Klocke, F., and Wirtz, H., "Improving Rapid Prototyping Processing Speeds by Adaptive Slicing," *Proceedings, Sixth European Conference on Rapid Prototyping and Manufacturing*, Dickens, P. M., ed., Nottingham, UK, July 1-3, 1997, pp. 31-36.

[Kulkarni95] Kulkarni, P., and Dutta, D., "Adaptive Sli cing for Parameterizable Surfaces for Layered Manufacturing," *Proceedings, ASME Design Engineering Technical Conference*, Azarm, S., *et al*., eds., Boston, Massachusetts, USA, September 17-20, 1995, DE-Vol. 82-1, pp.211-217.

[Kulkarni96] Kulkarni, P., and Dutta, D., "An Accurate Slicing Procedure for Layered Manufacturing," *Computer-Aided Design*, vol. 28, no. 9, September 1996, pp. 683-697.

[Merz94] Merz, R., Prinz, F. B., Ramaswami, K., Terk, M., and Weiss, L. E., "Shape Deposition Manufacturing," *Proceedings, Solid Freeform Fabrication Symposium*, Marcus, H. L., *et al*., eds., University of Texas at Austin, Austin, Texas, USA, August 8-10, 1994, pp. 1-8.

[O'Rourke94] O'Rourke, J., *Computational Geometry in C*, Cambridge University Press, 1994.

[Reeves97] Reeves, P. E., Dickens, P. M., Davey, N., and Cobb, R. C., "Surface Roughness of Stereolithography Models Using an Alternative Build Strategy," *Proceedings, Sixth European Conference on Rapid Prototyping and Manufacturing*, Dickens, P. M., ed., Nottingham, UK, July 1-3, 1997, pp. 85-94.

[Rock91a] Rock, S. J., and Wozny, M. J., "A Flexible File Format for Solid Freeform Fabrication," *Proceedings, Solid Freeform Fabrication Symposium*, Marcus, H. L., *et al.,* eds., University of Texas at Austin, Austin, Texas, USA, August 12-14, 1991, pp. 1-11.

[Rock91b] Rock, S. J., and Wozny, M. J., "Utilizing Topological Information to Increase Scan Vector Generation Efficiency," *Proceedings, Solid Freeform Fabrication*

Symposium, Marcus, H. L., *et al*., eds., University of Texas at Austin, Austin, Texas, USA, August 12-14, 1991, pp. 28-36.

[Rock92] Rock, S. J., and Wozny, M. J., "Generating Topological Information from a Bucket of Facets," *Proceedings, Solid Freeform Fabrication Symposium* , Marcus, H. L., *et al*., eds., University of Texas at Austin, Austin, Texas, USA, August 3-5, 1992, pp. 251-258.

[Sabourin96a] Sabourin, E., "Adaptive High-Precision Exterior, High-Speed Interior, Layered Manufacturing," M.S. Thesis, Virginia Polytechnic Institute and State University, Blacksburg, Virginia, USA, February, 1996.

[Sabourin96b] Sabourin, E., Houser, S. A., and Bøhn, J. H., "Adaptive Slicing Using Stepwise Uniform Refinement," *Rapid Prototyping Journal*, vol. 2, no. 4, 1996, pp. 20-26.

[Sabourin97] Sabourin, E., Houser, S. A., and Bøhn, J. H., "Accurate Exterior, Fast Interior Layered Manufacturing," *Rapid Prototyping Journal*, vol. 3, no. 2, 1997, pp. 44-52.

[Sachs97] Sachs, E., Allen, A., Honglin, G., Banos, J., Cima, M., Serdy, J., and Brancazio, D., "Progress on Tooling by 3D Printing; Conformal Cooling, Dimensional Control, Surface Finish and Hardness," *Proceedings, Solid Freeform Fabrication Symposium*, Bourell, D. L., *et al*., eds., University of Texas at Austin, Austin, Texas, USA, August 11-13, 1997, pp. 115-123.

[Sperling92] Sperling, L. H., *Introduction to Physical Polymer Science, 2 nd Edition*, John Wiley and Sons, Inc., 1992, pp. 467-487.

[Stratasys97] QuickSlice 5.0, Stratasys, Inc., Eden Prairie, Minnesota, USA, 1997.

[Suh94] Suh, Y. S., and Wozny, M. J., "Adaptive Slicing of Solid Freeform Fabrication Processes," *Proceedings, Solid Freeform Fabrication Symposium* , Marcus, H. L., *et al*., eds., University of Texas at Austin, Austin, Texas, USA, August. 8-10, 1994, pp. 404-411.

[Thomas96] Thomas, C. L., Gaffney, T. M., Kaza, S., and Lee, C. H., "Rapid Prototyping of Large Scale Aerospace Structures," *Proceedings, 1996 IEEE Aerospace Applications Conference,* Profet, R., chair, Aspen, Colorado, USA, February 4-11, 1996, Vol. 4, pp. 219-230.

[USPro96] US Product Data Association, *Initial Graphics Exchange Specification (IGES)* , version 5.3, IGES/PDES Organization, 1996.

[Vuyyuru94] Vuyyuru, P., Kirschman, C. F., Fadel, G., Baghi, A., and Jara-Almonte, C. C., " A NURBS-Based Approach for Rapid Product Realization," *Proceedings, Fifth International Conference on Rapid Prototyping* , Chartoff, R. P., *et al*., eds., University of Dayton, Dayton, Ohio, USA, June 12-15, 1994, pp. 229-240.

[Yardimici97] Yardimici, M. A., Hattori, T., Guceri, S.I., and Danforth, S.C., "Thermal Analysis of Fused Deposition," *Proceedings, Solid Freeform Fabrication Symposium*, Bourell, D. L., *et al*., eds., University of Texas at Austin, Austin, Texas, USA, August 11-13, 1997, pp. 689-698.

[Zheng97] Zheng, Y., and Newman, W. S., "Software Design Challenges for Computer-Aided Manufacturing of Laminated Engineering Materials (CAM-LEM)," *Proceedings, Sixth European Conference on Rapid Prototyping and Manufacturing*, Dickens, P. M., ed., Nottingham, UK, July 1-3, 1997, pp. 21-30.

APPENDIX A: GEOMETRIC PROOFS

As described in Section 2.5, Kulkarni and Dutta [Kulkarni95] [Kulkarni96] compute adaptive build layer thickness values to match the vertical surface curvature at a point *P* by assuming that the surface at *P* can be approximated by a sphere whose radius is equivalent to the vertical curvature at that point. Specifically, they site four possible configurations that must be handled when using this method (Figure A.1). This appendix provides derivations for the four independent expressions that were developed using the geometry shown in each of these configurations. These derivations were not presented in [Kulkarni95] [Kulkarni96].

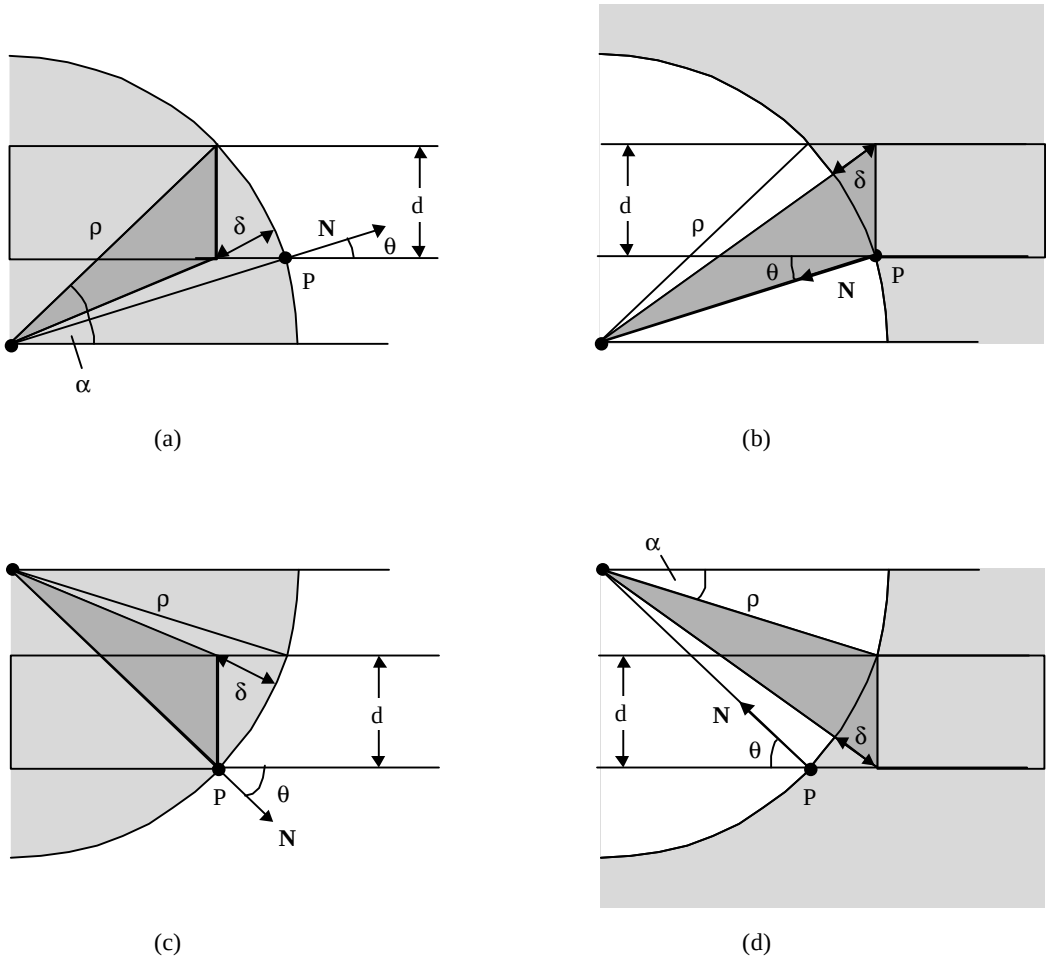

P:	a point on the part surface
N:	the surface normal at P
θ:	the angle that **N** makes to the horizontal
ρ:	the radius of curvature at P
δ:	the allowed cusp height
d:	the layer thickness to be computed

Figure A.1: Four possible configurations that may be encountered when using the build layer thickness approximation method developed by Kulkarni and Dutta; (a) convex curvature on upper hemisphere; (b) concave curvature on upper hemisphere; (c) convex curvature on lower hemisphere; and (d) concave curvature on lower hemisphere; [Kulkarni96]

Configuration (a):

By applying the law of cosines to the shaded triangle in Figure A.1a, equation (A.1) is produced,

$$(r - d)^2 = r^2 + d^2 - 2rd\cos(90 - a) \tag{A.1}$$

where (90 - a) is the included angle between sides r and d. Using the definition cos(90 - a) = sin a, (A.1) reduces to

$$r^2 - 2r\,d + d^2 = r^2 + d^2 - 2rd\sin a$$

which can be further simplified to obtain

$$d^2 - 2rd\sin a + (2r\,d - d^2) = 0 \tag{A.2}$$

It is clear that

$$r\sin a = d + r\sin q \tag{A.3}$$

By substituting (A.3) into (A.2) and simplifying, it can be shown that

$$d^2 + (2r\sin q)d - (2r\,d - d^2) = 0 \tag{A.4}$$

The build layer thickness d can now be determined using the quadratic equation:

$$d = \frac{-2r\sin q + \sqrt{4r^2\sin^2 q + 4(2r\,d - d^2)}}{2}$$

Finally, after simplifying,

$$\underline{\underline{d = -r\sin q + \sqrt{r^2\sin^2 q + 2r\,d - d^2}}} \tag{A.5}$$

Configuration (b):

By applying the law of cosines to the shaded triangle in Figure A.1b, equation (A.6) is produced,

$$(r + d)^2 = r^2 + d^2 - 2rd\cos(90 + q) \tag{A.6}$$

where $(90 + q)$ is the included angle between sides r and d. Using the definition $\cos(90 + q) = -\sin q$, (A.6) reduces to

$$r^2 + 2r\,d + d^2 = r^2 + d^2 + 2rd\sin q$$

which can be further simplified to obtain

$$d^2 + (2r\sin q)d - (2r\,d + d^2) = 0 \tag{A.7}$$

The build layer thickness d can now be determined using the quadratic equation:

$$d = \frac{-2r\sin q + \sqrt{4r^2\sin^2 q + 4(2r\,d + d^2)}}{2}$$

Finally, after simplifying,

$$\underline{\underline{d = -r\sin q + \sqrt{r^2\sin^2 q + 2r\,d + d^2}}} \tag{A.8}$$

Configuration (c):

By applying the law of cosines to the shaded triangle in Figure A.1c, equation (A.9) is produced,

$$(r - d)^2 = r^2 + d^2 - 2rd\cos(90 - q) \tag{A.9}$$

where (90 - q) is the included angle between sides r and d. Using the definition cos(90 - q) = sin q, (A.9) reduces to

$$r^2 - 2r\,d + d^2 = r^2 + d^2 - 2rd\sin q$$

which can be further simplified to obtain

$$d^2 - (2r\sin q)d + (2r\,d - d^2) = 0 \tag{A.10}$$

The build layer thickness d can now be determined using the quadratic equation:

$$d = \frac{2r\sin q - \sqrt{4r^2\sin^2 q - 4(2r\,d - d^2)}}{2}$$

Finally, after simplifying,

$$\underline{\underline{d = r\sin q - \sqrt{r^2\sin^2 q - 2r\,d + d^2}}} \tag{A.11}$$

Configuration (d):

By applying the law of cosines to the shaded triangle in Figure A.1d, equation (A.12) is produced,

$$(r + d)^2 = r^2 + d^2 - 2rd\cos(90 + a) \tag{A.12}$$

where $(90 + a)$ is the included angle between sides r and d. Using the definition $\cos(90 + a) = -\sin a$, (A.12) reduces to

$$r^2 + 2r\,d + d^2 = r^2 + d^2 + 2rd\sin a$$

which can be further simplified to obtain

$$d^2 + 2rd\sin a - (2r\,d + d^2) = 0 \tag{A.13}$$

It is clear that

$$r\sin a = r\sin q - d \tag{A.14}$$

By substituting (A.14) into (A.13) and simplifying, it can be shown that

$$d^2 - (2r\sin q)d + (2r\,d + d^2) = 0 \tag{A.15}$$

The build layer thickness d can now be determined using the quadratic equation:

$$d = \frac{2r\sin q - \sqrt{4r^2\sin^2 q - 4(2r\,d + d^2)}}{2}$$

Finally, after simplifying,

$$\underline{\underline{d = r\sin q - \sqrt{r^2\sin^2 q - 2r\,d - d^2}}} \tag{A.16}$$

VITA

My older twin sister and I were born in Washington, DC, on May 8, 1973. My parents saw to it that I would become independent (and stubborn) by conceiving two more daughters. When I wasn't sequestering myself in my room, doing homework, I was usually out playing on the soccer field or running around a large oval track. Through my schooling and athletics, I learned dedication and perseverance. I spent most of my childhood in Southeastern NY (Peekskill), but attended high school in the outskirts of Philadelphia, PA. I decided to matriculate at Virginia Tech because of its outstanding reputation in engineering, and because it was a seven hour drive from my parents. After earning a bachelor's degree in Aerospace Engineering, and gaining valuable work experience while building submarines at General Dynamics, Electric Boat Division in Groton, CT, I decided to pursue a Master's degree in Mechanical Engineering. Not wanting to leave Blacksburg, I remained at Virginia Tech where I was introduced to the world of CAD/CAM and rapid prototyping. I spent the summer of 1997 in Plantation, FL where I worked as an intern at Motorola, Land Mobile Products Center. Through my experiences I have discovered an appreciation for programming, and I plan to develop my skills in this area in my future endeavors.